

Mar 30th, 12:00 PM - 1:00 PM

A Comparison of In Vitro Studies Between Cobalt(III) and Copper(II) Complexes with Thiosemicarbazone Ligands to Treat Triple Negative Breast Cancer

Duaa R. Alajroush
Old Dominion University

Chloe B. Smith
Old Dominion University

Brittney F. Anderson
University of the Virgin Islands

Ifeoluwa T. Oyeyemi
University of Medical Sciences, Ondo

Stephen J. Beebe
Old Dominion University

See next page for additional authors

Follow this and additional works at: <https://digitalcommons.odu.edu/undergradsymposium>

 Part of the [Biochemistry Commons](#), [Cancer Biology Commons](#), and the [Molecular Biology Commons](#)

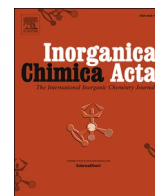
Alajroush, Duaa R.; Smith, Chloe B.; Anderson, Brittney F.; Oyeyemi, Ifeoluwa T.; Beebe, Stephen J.; and Holder, Alvin A., "A Comparison of In Vitro Studies Between Cobalt(III) and Copper(II) Complexes with Thiosemicarbazone Ligands to Treat Triple Negative Breast Cancer" (2024). *Undergraduate Research Symposium*. 5.

<https://digitalcommons.odu.edu/undergradsymposium/2024/sciences/5>

This Oral Presentation is brought to you for free and open access by the Undergraduate Student Events at ODU Digital Commons. It has been accepted for inclusion in Undergraduate Research Symposium by an authorized administrator of ODU Digital Commons. For more information, please contact digitalcommons@odu.edu.

Author Information

Duaa R. Alajroush, Chloe B. Smith, Brittney F. Anderson, Ifeoluwa T. Oyeyemi, Stephen J. Beebe, and Alvin A. Holder



Research paper

A comparison of *in vitro* studies between cobalt(III) and copper(II) complexes with thiosemicarbazone ligands to treat triple negative breast cancer

Duaa R. Alajroush^a, Chloe B. Smith^a, Brittney F. Anderson^b, Ifeoluwa T. Oyeyemi^{a,c}, Stephen J. Beebe^d, Alvin A. Holder^{a,*}

^a Department of Chemistry and Biochemistry, Old Dominion University 4501 Elkhorn Avenue, Norfolk, VA 23529, USA

^b Department of Biological Sciences, University of the Virgin Islands, 2 John Brewers Bay, St. Thomas, VI 00802, USA

^c Department of Biological Sciences, University of Medical Sciences, Ondo City, Nigeria

^d Frank Reidy Research Center for Bioelectrics, Old Dominion University, 4211 Monarch Way, Suite 300, Norfolk, VA 23508, USA



ARTICLE INFO

Keywords:

Triple negative breast cancer
Thiosemicarbazone
Cobalt(III) complex
Copper(II) complex
Apoptosis

ABSTRACT

Metal complexes have gained significant attention as potential anti-cancer agents. The anti-cancer activity of [Co(phen)₂(MeATSC)](NO₃)₃·1.5H₂O·C₂H₅OH **1** (where phen = 1,10-phenanthroline and MeATSC = 9-anthraldehyde-*N*(4)-methylthiosemicarbazone) and [Cu(acetylothTSC)Cl]Cl·0.25C₂H₅OH **2** (where acetylothTSC = (*E*)-*N*-ethyl-2-[1-(thiazol-2-yl)ethylidene]hydrazinecarbothioamide) was investigated by analyzing DNA cleavage activity. The cytotoxic effect was analyzed using CCK-8 viability assay. The activities of caspase 3/7, 9, and 1, reactive oxygen species (ROS) production, cell cycle arrest, and mitochondrial function were further analyzed to study the cell death mechanisms. Complex **2** induced a significant increase in nicked DNA. The IC₅₀ values of complex **1** were 17.59 μM and 61.26 μM in cancer and non-cancer cells, respectively. The IC₅₀ values of complex **2** were 5.63 and 12.19 μM for cancer and non-cancer cells, respectively. Complex **1** induced an increase in ROS levels, mitochondrial dysfunction, and activated caspases 3/7, 9, and 1, which indicated the induction of intrinsic apoptotic pathway and pyroptosis. Complex **2** induced cell cycle arrest in the S phase, ROS generation, and caspase 3/7 activation. Thus, complex **1** induced cell death in the breast cancer cell line via activation of oxidative stress which induced apoptosis and pyroptosis while complex **2** induced cell cycle arrest through the induction of DNA cleavage.

1. Introduction

Triple negative breast cancer (TNBC) originates from the outer (basal) layer of the breast ducts (i.e., myoepithelial cells) [1]. It represents about 15–20 % of breast cancer cases in young women under 40 years of age [2–5]. African American women are more likely to develop a triple negative breast tumor than people of other races [6,7]. TNBC tends to grow more aggressively and spread more quickly than most

other types of breast cancer [8]. Moreover, it represents 75 % of tumors in patients with BRCA1 gene mutation, leading to the dysregulation of cell cycle checkpoint, abnormal centrosome duplication, and genetic instability [9,10]. It is the most difficult breast cancer subtype to treat due to the absence of three receptors: estrogen, progesterone, and human epidermal growth factor receptor 2 (HER2) [11–13]. Therefore, therapeutic options for TNBC are limited, since hormonal and targeted therapies, such as tamoxifen (Nolvadex) and trastuzumab (Herceptin)

Abbreviations: acetylothTSC, (*E*)-*N*-ethyl-2-[1-(thiazol-2-yl)ethylidene]hydrazinecarbothioamide; CCK-8 assay, Cell Counting Kit-8; DMEM, Dulbecco's Modified Eagle Medium; DAPI, 4',6-diamidino-2-phenylindole; EMEM, Eagle's Minimum Essential Medium; EGF, Epidermal growth factor; ECAR, Extracellular acidification rate; ETC, Electron transport chain; FBS, Fetal bovine serum; FCCP, Carbonyl cyanide-4 (trifluoromethoxy) phenylhydrazone; HER2, Human epidermal growth factor receptor 2; LC DNA, Linear circular DNA; MeATSC, 9-anthraldehyde-*N*(4)-methylthiosemicarbazone; NAC, *N*-acetylcysteine; NC DNA, Nicked circular DNA; OCR, Oxygen consumption rate; Phen, 1,10-phenanthroline; ROS, Reactive oxygen species; RFP, Red fluorescent protein; Rot/AA, Rotenone/antimycin A; SC DNA, Supercoiled DNA; TNBC, Triple negative breast cancer; TSCs, Thiosemicarbazones; VIM, Vimentin; WST-8, [2-(2-methoxy-4-nitrophenyl)-3-(4-nitrophenyl)-5-(2,4-disulphophenyl)-2H-tetrazolium, monosodium salt]; z-VAD-FMK, benzyloxycarbonyl-Val-Ala-Asp-(*O*-methyl)-fluoromethylketone.

* Corresponding author.

E-mail address: aholder@odu.edu (A.A. Holder).

<https://doi.org/10.1016/j.ica.2023.121898>

Received 27 September 2023; Received in revised form 20 December 2023; Accepted 20 December 2023

Available online 22 December 2023

0020-1693/© 2023 Elsevier B.V. All rights reserved.

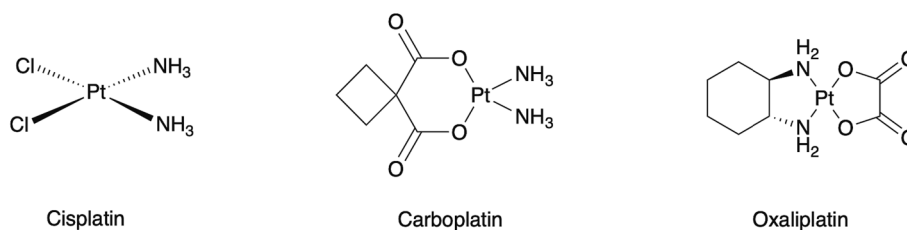


Fig. 1. Structures of cisplatin, carboplatin, and oxaliplatin.

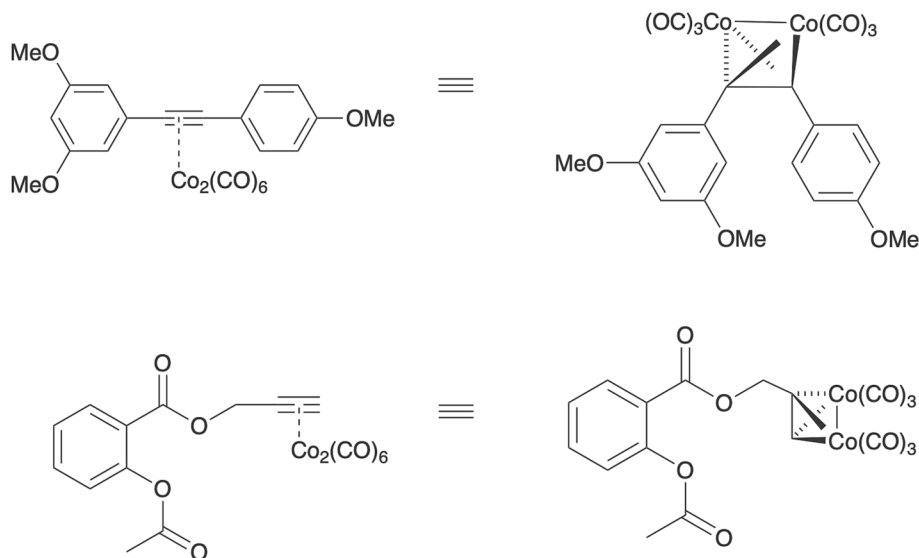


Fig. 2. Structures of hexacarbonyldicobalt complexes.

are ineffective [14–16]. Researchers are interested in synthesizing effective anti-cancer drugs because chemotherapy works best for this type of breast cancer [17].

Anti-cancer drugs interfere with cell division by disrupting DNA duplication or separation of newly formed chromosomes [18,19]. Metal-based compounds are a discrete class of chemotherapeutics used as antitumors and antiviral agents [20]. These metal-based compounds can be improved by changing the nature of the metal ion via its oxidation state or the number and type of ligands bound [21]. Cisplatin (see Fig. 1), a platinum-based drug that is the most widely used anti-cancer drug, has proven to be an effective chemotherapeutic drug for treating different types of cancer [22–24]. However, cisplatin has potentially dangerous side effects such as nephrotoxicity, which may lead to cisplatin-induced acute renal failure [25,26]. Other platinum-containing complexes, such as carboplatin and oxaliplatin (see Fig. 1), showed high anti-cancer activity [27–29]. Although carboplatin and oxaliplatin were successfully designed to reduce the side effects of cisplatin, their toxicity, and drug resistance still posed challenges to their therapeutic efficacy [29–31]. The clinical use of platinum-containing therapeutic drugs is limited due to inherent resistance and toxic side effects [32–34]. These limitations have prompted an increased interest in non-platinum metal complexes with anti-cancer effects [35].

The varied array of coordination numbers that metal complexes may have and their unique kinetic properties have long made them attractive alternatives to organic agents as they offer mechanisms of drug action which these agents cannot achieve [36]. Over the last few decades, research involving the biomedical application of transition metal complexes with ruthenium, titanium, or gallium metal centres has progressed in an effective manner, all in such a way that several complexes have entered clinical phase I and phase II studies [37–42]. For example, (imidazole-H)[*trans*-RuCl₄ (DMSO-S)(imidazole)], a ruthenium-based

complex has proven to be cytotoxic, as well as displayed selectivity for solid tumor metastasis, and has therefore been entered in phase I clinical trial [43]. Transition metal complexes of iron, cobalt, and gold metal centres have also been involved in preclinical research. Cobalt alkyl complexes were initially identified as a potential class of antitumor drugs in murine leukemia cells, and a series of hexacarbonyldicobalt complexes as shown in Fig. 2 have been identified that displayed significant anti-proliferative properties in multiple human tumor cell lines [36]. However, recently hexacarbonyldicobalt complexes such as hexacarbonyl[1,3-dimethoxy-5-((4'-methoxyphenyl)ethynyl)benzene]dicobalt have been found to induce apoptosis in BJAB lymphoma and Nalm-6 leukemia cells at low micromolar concentrations. This complex was reported not to have an effect on normal leukocytes as determined via *in vitro* studies, but it was active against vincristine and daunorubicin-resistant leukemia cell lines with *p*-glycoprotein-caused multidrug resistance [44].

The importance of ligands is related to their ability to interact with biological target sites, such as DNA, protein receptors, and enzymes [45–55]. Thiosemicarbazones (TSCs) have been attracting the attention of researchers for several years due to their biological properties [56–63]. Thiosemicarbazones can exist in two forms (thione-thiol), and they became popular due to their capacity to coordinate metal ions in the anionic or natural form [64–67]. The antitumor effect of thiosemicarbazones is connected to their ability to inhibit the ribonucleotide reductase enzyme, which is involved in the rate-limiting step of DNA synthesis, and their selectivity toward hormone-responsive cancers [68,69]. Moreover, thiosemicarbazones can kill cancer cells by the generation of reactive oxygen species (ROS), disruption of mitochondria function, and blockage of the G2/M phase in the cell cycle [70]. Thiosemicarbazones can also inhibit the topoisomerase II α enzyme, which increases growth rate and plays an important role in DNA replication as

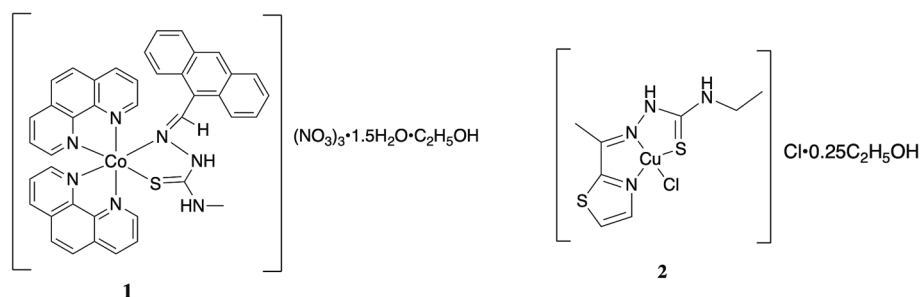


Fig. 3. Structures of complex 1 and complex 2, respectively.

it is required for condensation and segregation of chromosomes [68,71,72].

Cobalt is an important component of vitamin B₁₂ (cobalamin) in its +3 oxidation state and a necessary coenzyme of cell mitosis [42,73–80]. Moreover, cobalt plays different biological roles, such as involvement in the synthesis of red blood cells, formation of the myelin sheath in nerve cells, regulation of DNA synthesis, and growth and development [81]. The cytotoxicity of cobalt is related to its production of ROS and substitution of iron in metalloenzymes like prolyl 4-hydroxylase [82]. The cobalt(III) complex containing a thiosemicarbazone ligand, viz., [Co(2-acetylpyridine-4-phenyl-thiosemicarbazone)₂]Cl, has been previously reported and showed high anti-cancer activity against human skin (A431) and breast (MCF-7) cancer cell lines and efficiently inhibited cell survival even at low concentrations [83]. The cytotoxic effect of cobalt (III)-containing complexes against different cancer and non-cancer cell lines with their data are summarized in Table S1.

Copper is an essential element in the human body because it is required to activate many critical enzymes, form collagen, and stimulate hemoglobin synthesis [84]. Copper-containing complexes have displayed significant anti-cancer activity due to their high cytotoxicity [85]. The stability and viability of copper complexes are further increased when they coordinate with the thiosemicarbazones ligands [86]. Carcelli *et al.* reported the synthesis and use of six copper(II) complexes with salicylaldehyde thiosemicarbazone ligands in *in vitro* and *in vivo* studies. The complexes had IC₅₀ values in a low nanomolar range in multiple tumor cell lines [87]. Copper bis(thiosemicarbazone) complexes with methyl, phenyl, and hydrogen on a diketo-backbone were also cytotoxic in many human cancer cell lines with micromolar IC₅₀ values. Cell death was achieved through DNA cleavage and topoisomerase II α inhibition [88]. Copper(II)-containing complexes were previously reported and showed a good cytotoxic effect against different cancer and non-cancer cell lines as shown in Table S2.

As part of our efforts to fight cancer with the use of cobalt- and copper-containing thiosemicarbazone complexes, we have decided to focus on a cobalt(III) complex, [Co(phen)₂(MeATSC)](NO₃)₃·1.5H₂O·C₂H₅OH **1** [89] and a copper(II) complex, [Cu(acetylthTSC)Cl]Cl·0.25C₂H₅OH **2** [90] that are shown in Fig. 3. In our previous study, complex **1** was cytotoxic to mouse metastatic breast cancer cell line (4 T1-luc) [89]. Complex **2** was cytotoxic toward various colon cancer cell lines. It also showed a significant inhibition for human topoisomerase II α [90]. Herein, we investigated the cytotoxic effect of complex **1** and complex **2** on a human TNBC cell line, MDA-MB-231 VIM RFP, and a human non-cancer breast epithelial cell line, MCF-10A. Studies of induction of apoptosis and pyroptosis, generation of ROS, DNA cleavage activity, and cell cycle arrest, along with the effect on mitochondrial function were also discussed.

2. Experimental

2.1. Reagents

All chemicals and reagents were purchased from commercial sources

for *in vitro* studies with Co(III) and Cu(II) complexes. Eagle's Minimum Essential Medium (EMEM), fetal bovine serum (FBS), Dulbecco's Modified Eagle Medium (DMEM), and horse serum were obtained from Mediatech, Inc. (Manassas, VA). Cell Counting Kit-8 (CCK-8) assay kit was obtained from Dojindo. CellTiter-Glo® 2.0 assay, Caspase-Glo® 3/7 assay, Caspase-Glo® 9 assay, and Caspase-Glo® 1 Inflammasome assay kits were purchased from Promega Corporation (Madison, WI). CellROX® Green flow cytometry assay kit, CellEvent™ Caspase-3/7 Green flow cytometry assay kit, DAPI (4',6-diamidino-2-phenylindole) blue-fluorescent DNA stain, electrophoresis-grade low EEO agarose, boric acid, tris(hydroxymethyl)aminomethane (Tris), ethidium bromide, GeneRuler™ DNA Ladder, and 6x DNA dye were purchased from ThermoFisher Scientific. pUC18 DNA plasmid (2686 bp) was obtained from Bayou Biolabs. The Seahorse XF Cell Mito Stress Test kit (Agilent, 103010-100) was purchased from Agilent Technologies.

2.2. Synthesis of complexes

The cobalt(III) complex, [Co(phen)₂(MeATSC)](NO₃)₃·1.5H₂O·C₂H₅OH **1** was synthesized as reported by Beebe *et al.* [89]; while the copper(II) complex, [Cu(acetylthTSC)Cl]Cl·0.25C₂H₅OH **2** was synthesized as reported by Sandhaus *et al.* [90].

2.3. DNA cleavage activity

The DNA cleavage activity of complexes was determined by monitoring the conversion of supercoiled plasmid pUC18 DNA (SC DNA) to nicked circular (NC DNA) or linear circular (LC DNA) by using agarose gel electrophoresis. Mixtures of 50 μM DNA and different concentrations of the complexes, with a total reaction volume of 100 μL , were incubated for 4 h and 24 h at 37 °C. These mixtures were also photolyzed at 740 nm for 4 h. The control solution has only DNA, while the samples have DNA with complexes. After incubation or irradiation, loading buffer (90 mM Tris, 90 mM boric acid, pH 8) was added, the mixtures were immediately loaded onto 0.8 % agarose gel at 104 V for 1.5 h. The agarose gels were then stained with 1.0 mg ml⁻¹ ethidium bromide aqueous solution for 1 h and photographed *via* UV illumination.

2.4. Cell culture

2.4.1. MDA-MB-231 VIM RFP cell line

MDA-MB-231 VIM (vimentin) RFP (red fluorescent protein) reporter TNBC cell line is fibroblast-like breast adenocarcinoma cell which was isolated from the pleural effusion of a 51-year-old, white, female TNBC cells. The MDA-MB-231 VIM RFP cells were obtained from American Type Culture Collection (ATCC). These cells were cultured in Eagle's Minimum Essential Medium (EMEM) that was supplemented with 10 % fetal bovine serum (FBS), 0.01 mg ml⁻¹ human recombinant insulin, and 10 μg ml⁻¹ blasticidin S HCl, 1 % penicillin/streptomycin, and incubated at 37 °C in a 5 % CO₂ atmosphere.

2.4.2. MCF-10A cell line

MCF-10A cells (non-tumorigenic human cell line from human breast epithelial cells) were obtained from American Type Culture Collection (ATCC). MCF-10A cells were cultured in Dulbecco's Modified Eagle Medium (DMEM) with 5 % horse serum, 20 ng ml⁻¹ epidermal growth factor (EGF), 0.5 µg ml⁻¹ hydrocortisone, 100 ng ml⁻¹ cholera toxin, 10 µg ml⁻¹ insulin, and 1 % penicillin/streptomycin, and incubated at 37 °C in a 5 % CO₂ atmosphere.

2.5. Cytotoxicity study

All cells were seeded in a 96-well clear-bottom plate at a concentration of 1.5 × 10⁴ cells/well. Complex 1, complex 2, and cisplatin were added to the cells at different concentrations (0–100 µM). Following the administration of the drugs, three plates were incubated for 24, 48, and 72 h, respectively. After incubation, the cells were assayed for viability using CCK-8 assay by adding the WST-8 reagent, followed by measuring the absorbance at 450 nm. To measure cell viability using the ATP assay, the CellTiter-Glo® 2.0 reagent was added after treating the cells with complexes. Then the plate was incubated at room temperature for 10 min to stabilize the luminescent signal. The luminescence signal was measured by using a microplate reader (Spectra Max i3). Origin 7.0 software was used to analyze the data and determine the IC₅₀ values.

To examine the effect of caspase 3/7 activity and ROS production on cell viability, cells were pre-incubated with 20 µM of benzyloxycarbonyl-Val-Ala-Asp-(O-methyl)-fluoro-methyl ketone (z-VAD-FMK) and different concentrations, in range (500–5000 µM), of N-acetylcysteine (NAC), respectively, for 2 h before the addition of complexes. WST-8 reagent was then added after 72 h incubation with the complexes; then the absorbance at 450 nm was read 1 h later.

2.6. Cell death mechanism studies

2.6.1. Reactive oxygen species (ROS) production

MDA-MB-231 VIM RFP cells were plated at a 3 × 10⁵ cells/mL concentration and treated with the IC₅₀ values of complex 1 and complex 2. The ROS level was then measured at various time courses by adding the CellROX® detection reagent at a final concentration of 500 nM. The samples were incubated for 30–60 min at 37 °C, 5 % CO₂, and protected from light. Finally, the vimentin-red fluorescent protein (VIM-RFP) of cells and CellROX® green fluorescence were read at 532/588 and 508/525 nm, respectively by using a Miltenyi MacsQuant Analyzer 10 flow cytometer.

2.6.2. Detection of apoptotic cell death

2.6.2.1. Caspase 3/7 activity. MDA-MB-231 VIM RFP cells were plated at a concentration of 3 × 10⁵ cells/mL and incubated for 24 h. The cells were treated with the IC₅₀ values of complex 1, complex 2, and cisplatin. The CellEvent™ Caspase-3/7 green reagent (2 µL) was added at different time points to 100 µL of samples; then the samples were incubated for 25 min at 37 °C at 5 % CO₂ and protected from light. The VIM-RFP in cells and the caspase 3/7 green fluorescent were collected at 532/588 and 511/533 nm, respectively by flow cytometry.

To study the relationship between apoptosis and ROS production, caspase 3/7 activity was evaluated in the presence and absence of NAC. The cells were plated in triplicate on 96-well plates (1.5 × 10⁴ cells/100 µL). Cells were pre-incubated with 3000 µM of NAC for 2 h before treatment with the IC₅₀ values of complexes. Caspase-Glo® 3/7 reagent was added to each well according to the manufacturer's instructions. The contents were gently mixed using a plate shaker at 300 rpm for 30 s, and the plate was incubated for 35 min at room temperature. Then the caspase 3/7 activity was measured at different times by reading the luminescence through a microplate reader.

2.6.2.2. Caspase 9 activity. Caspase 9 activity was analyzed to investigate the apoptotic pathways induced by the complexes to kill cancer cells since caspase 9 is involved in the intrinsic pathway. Caspase-Glo® 9 assay kit was used to study caspase 9 activity. The MDA-MB-231 VIM RFP cancer cells were seeded on a 96-well plate (1.5 × 10⁴ cells/well) in 100 µL of medium. The cells were treated with the IC₅₀ values of complex 1 and complex 2. Then the reagent of the assay was added to each sample, and the reaction mixtures were mixed by a plate shaker at 300–500 rpm for 30 s. The luminescence was read in a microplate reader after 1 h incubation at room temperature.

2.6.3. Detection of pyroptosis (caspase 1 activity)

Caspase-Glo® 1 Inflammasome assay was used to detect caspase 1 activity as a biomarker of inflammasome activity. The MDA-MB-231 VIM RFP cancer cells were plated at 1.5 × 10⁴ cells/100 µL in a 96-well plate; then the cells were treated with the IC₅₀ values of complex 1 and complex 2. The Caspase-Glo® 1 Inflammasome reagent was added to each well at different incubation times. The cell contents were mixed by a plate shaker at 300–500 rpm for 30 s and incubated at room temperature for 1 h. Finally, the caspase 1 activity was measured by reading the luminescence by using a microplate reader.

2.6.4. Mitochondrial function studies by the Seahorse XF Analyzer

The MDA-MB-231 VIM RFP cells were plated at a density of 2 × 10⁴ cells/80 µL in the Seahorse XF cell culture 8-well microplate and incubated overnight at 37 °C, 5 % CO₂. Then the cells were treated with two concentrations of complex 1. After 1 h of treatment, the Seahorse XF DMEM medium was added to the cells; then the cells were incubated in a non-CO₂ incubator for 60 min before starting the assay. The remaining steps were carried out according to the manufacturer protocol for the Seahorse XF Cell Mito Stress Test kit by adding four compounds (oligomycin, FCCP, rotenone, and antimycin A) at a constant concentration to the injection ports on the sensor cartridge. The Seahorse Extracellular Flux Analyzer Mini (SH-XFA; Agilent Technologies, USA) was set up for running the mitochondrial stress test assay. The data were analyzed using the Agilent Cell Analysis website; then processed by using Origin 7.0 software.

2.6.5. Cell cycle analysis

The cell cycle was evaluated by flow cytometry using DAPI staining on a flow cytometer. The cancer MDA-MB-231 VIM RFP cells were plated at a concentration of 1 × 10⁶ cells/mL in a 6-well plate, treated with the IC₅₀ value of complex 2 for 24 h. Then cells were washed in phosphate-buffered saline (PBS), resuspended with ice-cold 70 % EtOH, stored in the fixative at 4 °C for 2 h. Then cells were washed in PBS, resuspended in staining solution. Experiments were performed in triplicate. G1, S, and G2 fractions were quantified with the FlowJo software.

2.7. Statistical analysis

The FlowJo software was used for analyzing flow cytometric data. Origin 7.0 software was used to draw the curves of cytotoxic studies and determine the IC₅₀ values. ImageJ software was used to analyze the bands in the agarose gel electrophoresis. GraphPad Prism 9 software was used for statistical analyses namely one-way and/or two-way analysis of variance between groups. All experiments were conducted at least three times and data were expressed as mean ± standard error (S.E.). Asterisks represent P values of <0.05 "**", <0.01 "***", <0.001 "****", <0.0001 "*****".

3. Results and discussion

3.1. DNA cleavage studies

DNA is one of the main targets for transition metal complexes [91]. The cleaving efficacy of the complexes was assessed by their ability to

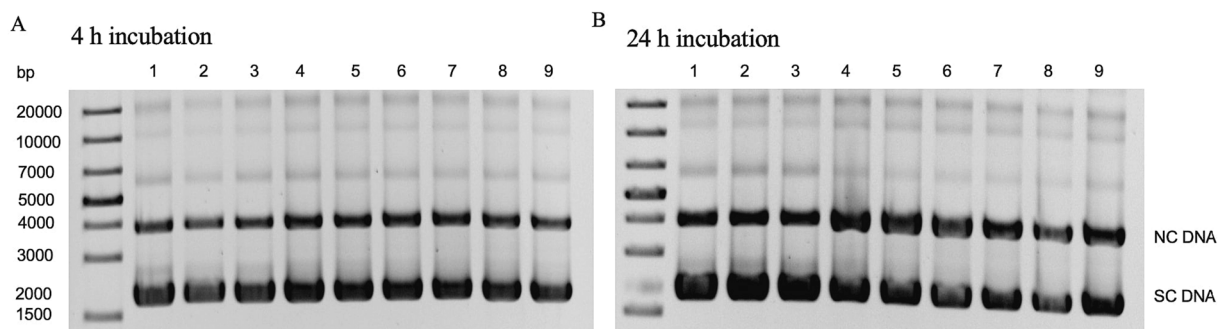


Fig. 4. Agarose gels show the DNA cleavage activity of complex 1 at 4 h (A) and 24 h (B) incubation. Lane 1: pUC18 DNA; lanes 2–9: pUC18 DNA with 10, 20, 40, 50, 60, 80, 90, and 100 μM of complex 1. The mixtures of 50 μM DNA and different concentrations of the complex were incubated for 4 and 24 h at 37 $^{\circ}\text{C}$. The samples were loaded onto 0.8 % agarose gel at 104 V for 1.5 h. Gels were then stained in 1.0 mg ml^{-1} ethidium bromide for 1 h and photographed with UV illumination. Data were analyzed by using ImageJ software.

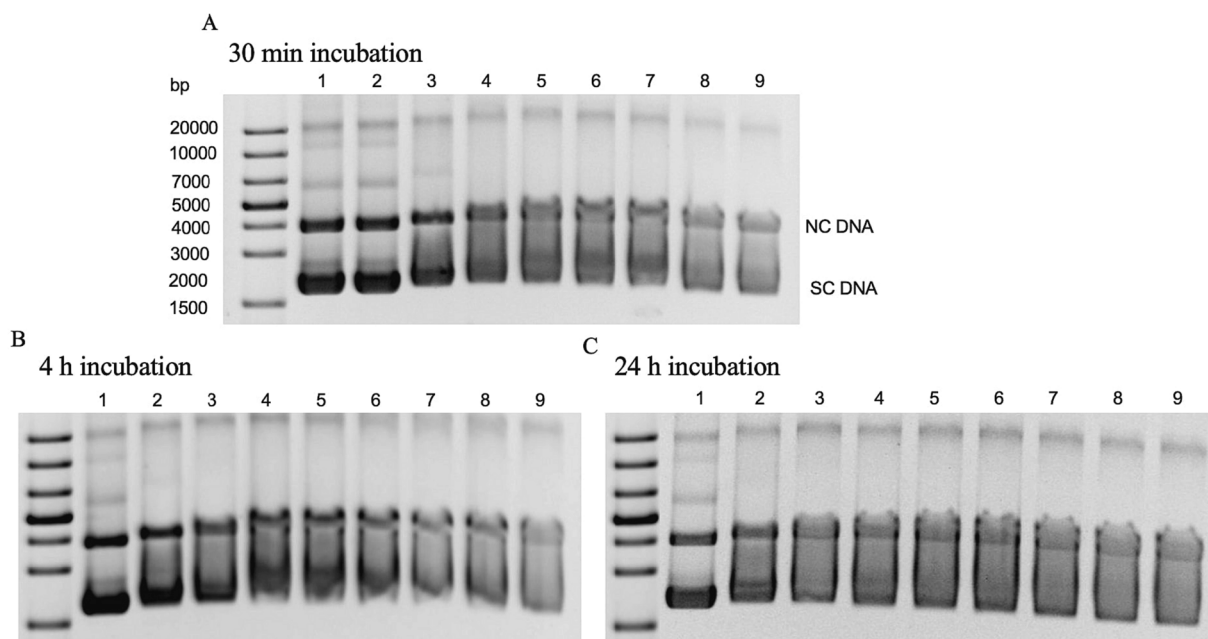


Fig. 5. Agarose gels show the DNA cleavage activity of complex 2 at 30 min (A), 4 h (B), and 24 h (C) incubation. Lane 1: pUC18 DNA; lanes 2–9: pUC18 DNA with 10, 20, 40, 50, 60, 80, 90, and 100 μM of complex 2. The samples were incubated for 30 min, 4 h, and 24 h at 37 $^{\circ}\text{C}$, then loaded onto 0.8 % agarose gel at 104 V for 1.5 h. Gels were then stained in 1.0 mg ml^{-1} ethidium bromide and photographed with UV illumination. Data were analyzed by using ImageJ software.

convert the supercoiled pUC18 DNA to its relaxed form by agarose gel electrophoresis. As shown in Fig. 4, upon incubation of plasmid pUC18 DNA (50 μM) with complex 1 (10–100 μM) for 4 and 24 h, there was a

decrease in the amount of supercoiled DNA and a concentration-dependent increase in the amount of nicked or relaxed circular DNA. There was an increase in the quantity of NC DNA after 24 h incubation

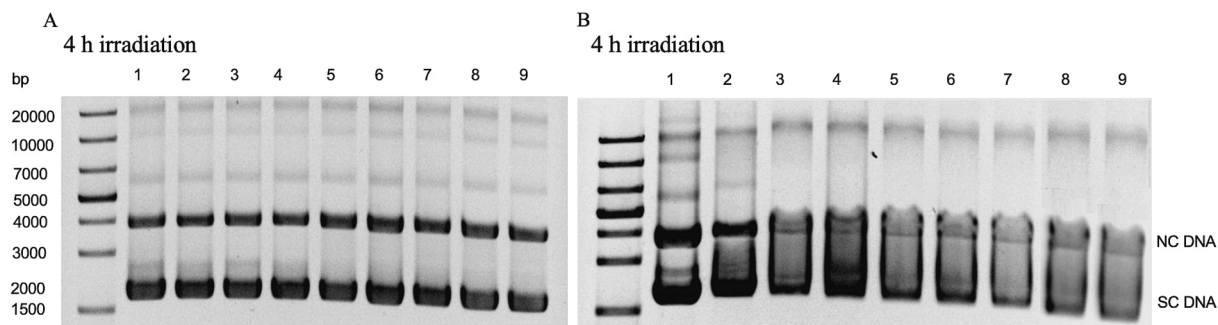


Fig. 6. Agarose gels show the DNA photocleavage activity of complex 1 (A) and complex 2 (B) after 4 h irradiation at 740 nm. Lane 1: pUC18 DNA without light; lane 2: pUC18 DNA with light; Lanes 3–9: pUC18 DNA with 10, 20, 40, 50, 60, 80, and 100 μM of the complexes. The samples were photolyzed at 740 nm for 4 h. After irradiation, the samples were immediately loaded onto 0.8 % agarose gel at 104 V for 1.5 h. Gel electrophoresis was conducted in the presence of ethidium bromide and photographed with UV illumination. Data were analyzed by using ImageJ software.

Table 1

Cytotoxic effects of complex 1, complex 2, and cisplatin via IC_{50} values on MDA-MB-231 VIM RFP and MCF-10A cells at different times.

Complexes	$IC_{50}/\mu\text{M}$			
	Cancer MDA-MB-231 VIM RFP			Non-cancer MCF-10A
	24 h	48 h	72 h	72 h
1	32.95 ± 1.8	20.83 ± 1.7	17.59 ± 1.1	61.26 ± 1.2
2	13.25 ± 0.8	7.17 ± 1.2	5.63 ± 1.2	12.19 ± 1.7
Cisplatin	28.13 ± 2.4	24.73 ± 2.6	22.17 ± 1.8	31.87 ± 2.0

compared to the 4 h incubation. The data indicate that DNA cleavage by complex 1 is time-dependent. The DNA cleavage could be a result of the inhibition of topoisomerase activity. Complex 1 had previously been reported to have shown topoisomerase inhibition activity [89]. As reported in the literature, inhibitors of topoisomerase can induce cytotoxicity by preventing the resealing of nicks in the DNA which leads to the accumulation of DNA breaks, inhibition of DNA replication, and ultimately cell death [92].

When compared to complex 1, complex 2 showed more significant DNA cleavage activity at 30 min, 4 h, and 24 h incubation as shown in Fig. 5. The observed DNA cleavage is also time-dependent as the quantity of nicked DNA increased with incubation time. Complex 2 was previously reported as a poison inhibitor of human topoisomerase II α [90]; and in this study, it is also possible that complex 2 can directly bind and cleave DNA. Interestingly, mixed-ligand copper(II)-phenolate complexes ($[\text{Cu}(\text{tdp})\text{ClO}_4] \cdot 0.5\text{H}_2\text{O}$ (where tdp is a tetradentate ligand, 2-[(2-(2-hydroxyethylamino)ethylimino)methyl]phenol, and the mixed ligand complexes $[\text{Cu}(\text{tdp})(\text{diimine})]^+$ (where diimine = 2,2'-bipyridine (bpy), 1,10-phenanthroline (phen), 3,4,7,8-tetramethyl-1,10-phenanthroline (tmp), and dipyrido-[3,2-d:2',3'-f]-quinoxaline (dpq)) have been reported to interact with DNA and cleave pBR322 supercoiled DNA [93].

During photocleavage of DNA (as shown in Fig. 6), complexes 1 and 2 showed higher DNA cleavage activity after 4 h when compared to 4 h incubation without light. This shows that complexes 1 and 2 can photocleave DNA, whereby complex 2 being the more efficient of the two complexes. It must be noted that complex 2 has a UV-visible spectrum that shows a d-d transition with a molar extinction coefficient value of $182 \text{ M}^{-1} \text{ cm}^{-1}$ at 624 nm, but also with a significant absorption at 740 nm [90].

Metal complexes are prone to the photochemical production of toxic reactive oxygen species due to their easy redox characteristics [94–96]. The increase in toxicity upon irradiation makes complexes potentially useful as photodynamic therapy (PDT) agents [97]. It was reported that complexes, $[\text{Co}(\text{phen})_2(\text{L})]^{3+}$ (where L = IP = imidazo[4,5-f][1,10]phenanthroline) and PIP = 2-phenylimidazo[4,5-f][1,10]phenanthroline) were efficient photosensitizers for strand scissions in plasmid DNA, which was due to their efficient DNA photocleavage in the presence of light [99]. In the

same vein, two Cu(II) complexes, $[\text{Cu}(\text{acac})(\text{dpq})\text{Cl}]$ and $[\text{Cu}(\text{acac})(\text{dppz})\text{Cl}]$ (where acac = acetylacetonate, dpq = dipyrido[3,2-d:20,30-f] quinoxaline, and dppz = dipyrido[3,2-a:20,30-c] phenazine) have been reported to show a good binding propensity to calf thymus DNA and an efficient DNA cleavage activity on natural light or UV-A (365 nm) irradiation through the generation of singlet oxygen as a reactive species [99]. Interestingly, $[\text{Cu}(\text{tdp})(\text{dpq})]^+$ was reported to display efficient photonuclease activity through double-strand DNA breaks upon irradiation with 365 nm light through a mechanistic pathway involving hydroxyl radicals [93].

3.2. Cytotoxicity evaluations

The cytotoxicity of complexes 1 and 2 against the cancer MDA-MB-231 VIM RFP and non-cancer MCF-10A cell lines was evaluated using CCK-8 assay which measures cell viability. The cells were treated with different concentrations (0–100 μM) of complex 1, complex 2, and cisplatin for 24, 48, and 72 h. Table 1 shows a tabulation of the IC_{50} values in MDA-MB-231 VIM RFP and MCF-10A cells with complexes 1 and 2 along with cisplatin as a control. A significant decrease in cell viability of MDA-MB-231 VIM RFP cells was observed following incubation with either of the two complexes as shown in Figs. S1, S2, and 7A. The IC_{50} values for complex 1 in MDA-MB-231 VIM RFP cancer cells were 32.95 ± 1.8 , 20.83 ± 1.7 , and $17.59 \pm 1.1 \mu\text{M}$ for 24, 48 and 72 h of incubation, respectively. The IC_{50} values for complex 2 were 13.25 ± 0.8 , 7.17 ± 1.2 , and $5.63 \pm 1.2 \mu\text{M}$ for 24, 48, and 72 h of incubation, respectively, while cisplatin showed IC_{50} values of 28.13 ± 2.4 , 24.73 ± 2.6 , and $22.17 \pm 1.8 \mu\text{M}$ following 24, 48, and 72 h incubation, respectively. The two complexes had lower IC_{50} values when compared to cisplatin at 48 and 72 h incubation. This implies that the complexes were more toxic to the cancer cell line and would be more efficient against TNBC when compared to cisplatin. Complex 2, however, showed the highest cytotoxic effect as evidenced by its low IC_{50} value.

To confirm the CCK-8 results, the ATP assay was utilized to determine the number of viable cells in the culture, which is directly proportional to the amount of ATP present. The IC_{50} values for complex 1, complex 2, and cisplatin at 72 h incubation in MDA-MB-231 VIM RFP cells were 18.13 ± 1.6 , 6.35 ± 1.4 , and $23.34 \pm 1.9 \mu\text{M}$, respectively as determined from Fig. S3. This is comparable to the results of the CCK-8 assay.

The cytotoxic effect of the complexes and cisplatin was evaluated in the non-cancer breast cell line, MCF-10A. As determined from Fig. 7B, the IC_{50} values of complex 1, complex 2, and cisplatin were $61.26 \pm 1.2 \mu\text{M}$, 12.19 ± 1.7 , and $31.87 \pm 2.0 \mu\text{M}$, respectively at 72 h incubation. This showed that complex 1 had a higher IC_{50} in the MCF-10A cell line when compared to cisplatin and compared to its IC_{50} in MDA-MB-231 VIM RFP cells. This implies that complex 1 is selectively cytotoxic to the breast cancer cell line but is not as toxic as cisplatin. Complex 2 on the other hand had a lower IC_{50} value in MCF-10A compared to

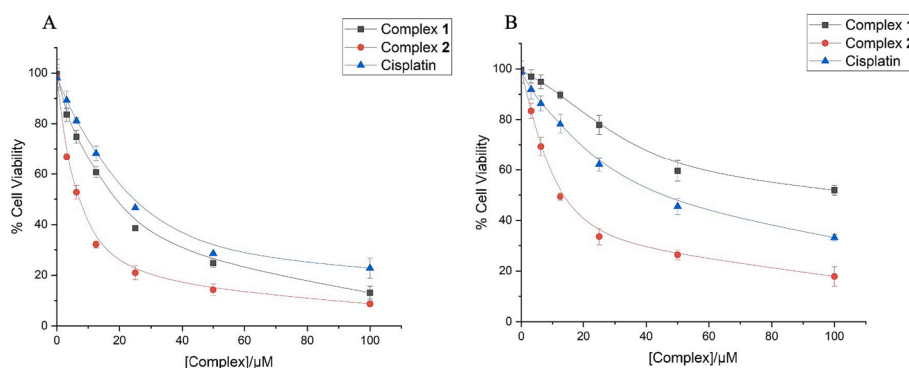


Fig. 7. A plot of the percentage of MDA-MB-231 VIM RFP (A) and MCF-10A (B) cell viability versus concentration of complex 1, complex 2, and cisplatin at 72 h incubation.

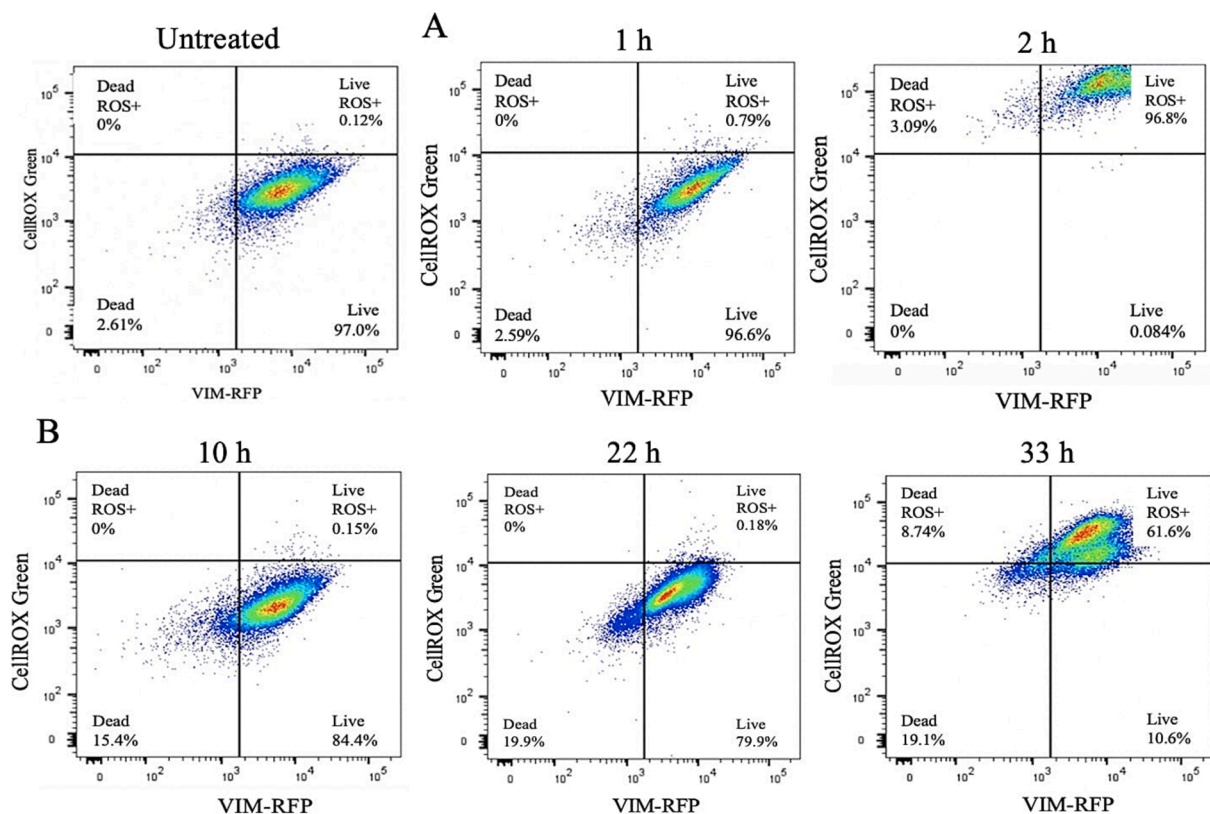


Fig. 8. ROS generation in the MDA-MB-231 VIM RFP cells after treatment with complex 1 ($IC_{50} = 17.5 \mu\text{M}$) (A) and complex 2 ($IC_{50} = 5.6 \mu\text{M}$) (B) at different time points using flow cytometry. The cells were seeded at a concentration of 3×10^5 cells/mL for 24 h before the treatment with the IC_{50} values of complexes. Then, 2 μL of the reagent was added at different time courses. Representative cell populations are shown with the fluorescence resulting from CellROX® at 508/525 nm, y-axis, and VIM-RFP at 532/588 nm, x-axis. Flow cytometry was used for data acquisition and FlowJo software was used for data analysis.

cisplatin, although slightly higher than its IC_{50} in MDA-MB-231 VIM RFP cells. This shows that it is toxic to both breast cancer and normal cell lines. In addition, the cytotoxic effect of DMSO, which was used to dissolve the complexes was investigated by using the CCK-8 assay. The MDA-MB-231 VIM RFP cells were treated with different concentrations of DMSO and incubated for 24, 48, and 72 h. The results did not show any cytotoxic effect for DMSO toward the cells as shown in Fig. S4.

3.3. Cell death mechanism evaluations

3.3.1. Role of ROS generation in cell death

Anti-cancer drugs can suppress cancer cell growth by ROS production [100]. A high level of ROS can inhibit cancers in different ways, including the oxidative damage of proteins, lipids, and DNA or by induction of some regulated cell death mechanisms like apoptosis and necroptosis as well as autophagy [101–103]. The formation of ROS was evaluated by the CellROX® Green flow cytometry assay kit where the reagent binds to DNA and gives green fluorescence under an oxidation state. When incubated with the IC_{50} value of complex 1, essentially all

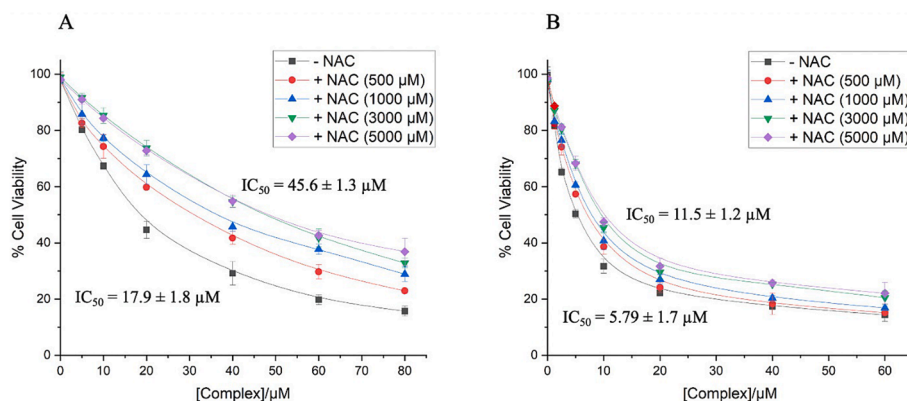


Fig. 9. The effect of ROS production on MDA-MB-231 VIM RFP cell viability after treatment with complex 1 (A) and complex 2 (B) in the presence and absence of the antioxidant, NAC. Cells were seeded at 1.5×10^4 cells per well for 24 h before the addition of different concentrations of NAC. After 2 h incubation with NAC, the complexes were administrated, and WST-8 reagent was added at 72 h of incubation with drugs. Graphs represent $n = 3$ replicates of data with plates. Data were analyzed by using Origin 7.0 software.

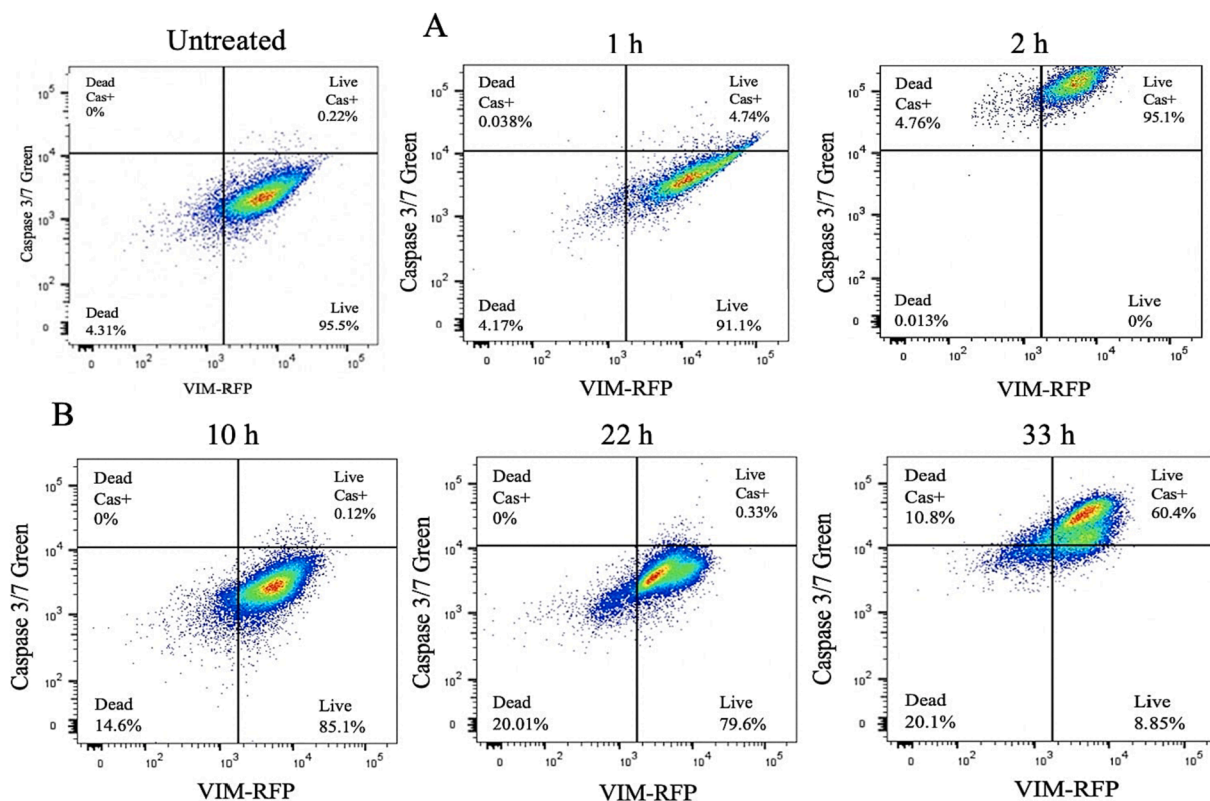


Fig. 10. Caspase 3/7 activity in the MDA-MB-231 VIM RFP cells after treatment with complex 1 ($IC_{50} = 17.5 \mu\text{M}$) (A) and complex 2 ($IC_{50} = 5.6 \mu\text{M}$) (B) at different time points. The cells were seeded at a concentration of 3×10^5 cells/mL following the treatment with the IC_{50} values of complexes. Then, 2 μL of the caspase 3/7 reagent was added at different time courses. The graph shows the population of cells that were activated by caspase 3/7 through collecting the RFP fluorescent at 532/588 and the caspase 3/7 green fluorescent at 511/533 nm by flow cytometry. FlowJo software was used for analyzing flow cytometric data. (For interpretation of the references to colour in this figure legend, the reader is referred to the web version of this article.)

cells were ROS positive at 2 h of treatment as shown in Fig. 8A. This is consistent with previous reports that cobalt-containing complexes induced ROS in cancer cells, such as the cobalt(III) Schiff base complexes, viz., $\text{Co}(\text{Ph-acacen})(\text{HA})_2](\text{ClO}_4)$ and $[\text{Co}(\text{Ph-acacen})(\text{DA})_2]\text{ClO}_4$ (where Ph-acacen = 1-phenyl butane-1,3-dione, DA = dodecyl amine, and HA = heptylamine) in breast MCF-7 and lung A549 cancer cells [104–106]. Complex 2 showed an increase in ROS level between 22 and 33 h of treatment as shown in Fig. 8B. Copper-containing complexes have been reported to induce ROS production in cancer cells [107], including copper(II) complexes with sodium salts of 3-formyl-4-hydroxybenzenesulfonic acid thiosemicarbazones (or sodium 5-sulfonate-salicylaldehyde thiosemicarbazones) [108], copper pyridine benzimidazole complexes in the lung A549 cell line [109], and copper (II) complexes of *N*-salicyl-*L*-tryptophan and 1,10-phenanthroline as ligands in cervical HeLa and breast MCF-7 cancer cells [110]. On the other hand, cisplatin was studied as a control and did not show any ROS production up to 48 h after treatment as shown in Fig. S5.

To determine the effect of ROS production on cell viability, a cell viability assay was carried out in the presence and absence of *N*-acetylcysteine (NAC). NAC in our body is converted to *L*-cysteine, which is converted to reduced glutathione in the liver [111]. Glutathione is an important antioxidant in the body that protects cells from oxidants [112]. Different concentrations of NAC were used in the range, 500–5000 μM , to determine the optimal final concentration required to inhibit ROS production in MDA-MB-231 VIM RFP cells. As shown in Fig. 9A, there was a dose-dependent increase in the survival of the cancer cells with increasing concentrations of NAC. Table S3 shows a tabulation of the IC_{50} values of complexes 1 and 2 in the presence and absence of various concentrations of NAC. The IC_{50} values at 3000 and 5000 μM of NAC were the same at 45.6 μM , so the optimal concentration

that is required to protect the MDA-MB-231 VIM RFP cells from oxidants is 3000 μM . At this concentration, the IC_{50} value of complex 1 was doubled to $45.6 \pm 1.3 \mu\text{M}$ compared to $17.9 \pm 1.8 \mu\text{M}$ in the absence of NAC. These data indicate that complex 1 induced ROS-dependent cell death mechanism. Similarly, there was a dose-dependent increase in the survival of the cancer cells with increasing concentrations of NAC after treatment with complex 2 as shown in Fig. 9B. The survival of cells was enhanced by about 15–20 % in the presence of 3000 μM of NAC.

3.3.2. Apoptotic mode of cell death

3.3.2.1. Caspase 3/7 activity. Most common mechanisms induced by anti-cancer drugs for suppressing cancer often involve modulation of signal transduction pathways, which leads to changes in gene expression, cell cycle arrest, and/or apoptosis [113]. Apoptosis is a programmed cell death mechanism that is activated primarily through two signaling pathways: receptor-dependent (extrinsic) and mitochondria-dependent (intrinsic) [114–116]. Both pathways activate caspase 3/7, which can be detected by the CellEvent™ Caspase-3/7 Green flow cytometry assay kit. The results of the control (untreated cells) did not show any caspase activity, and most cells were alive. As shown in Fig. 10A, caspase 3/7 was activated between the first and second hour after treatment with the IC_{50} value (17.59 μM) of complex 1. This aligns with a previous report that complex 1 induced caspase 3/7 activity in a concentration-dependent manner in cancer breast 4 T1-luc cells [89]. Complex 2 did not show caspase activity at 10 and 22 h of treatment as shown in Fig. 10B. Caspase 3/7 was activated at 33 h of treatment, suggesting that DNA cleavage eventually led to complex 2-induced apoptosis later at the 33-hour time point. This is in line with the previous report of a copper(II) complex inducing DNA cleavage, cytotoxicity, and

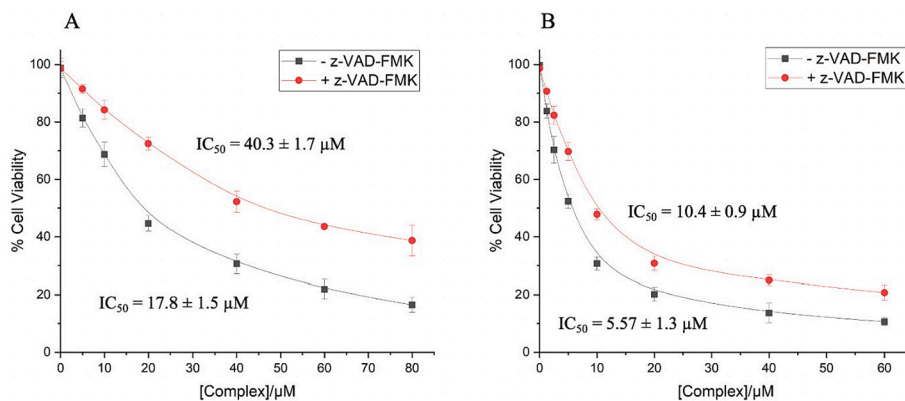


Fig. 11. The effect of caspase activation on cell viability after treatment of MDA-MB-231 VIM RFP cancer cells with complex 1 (A) and complex 2 (B) in the presence and absence of caspase inhibitor, z-VAD-FMK. Cells were seeded at 1.5×10^4 cells per well for 24 h before the addition of 20 μM of z-VAD-FMK, following the treatment after 2 h preincubation. Viability was assessed after 72 h of incubation with drugs. Graphs represent $n = 3$ replicates of data with plates being 1 h post incubation with WST-8 reagent. Data were analyzed by using Origin 7.0 software.

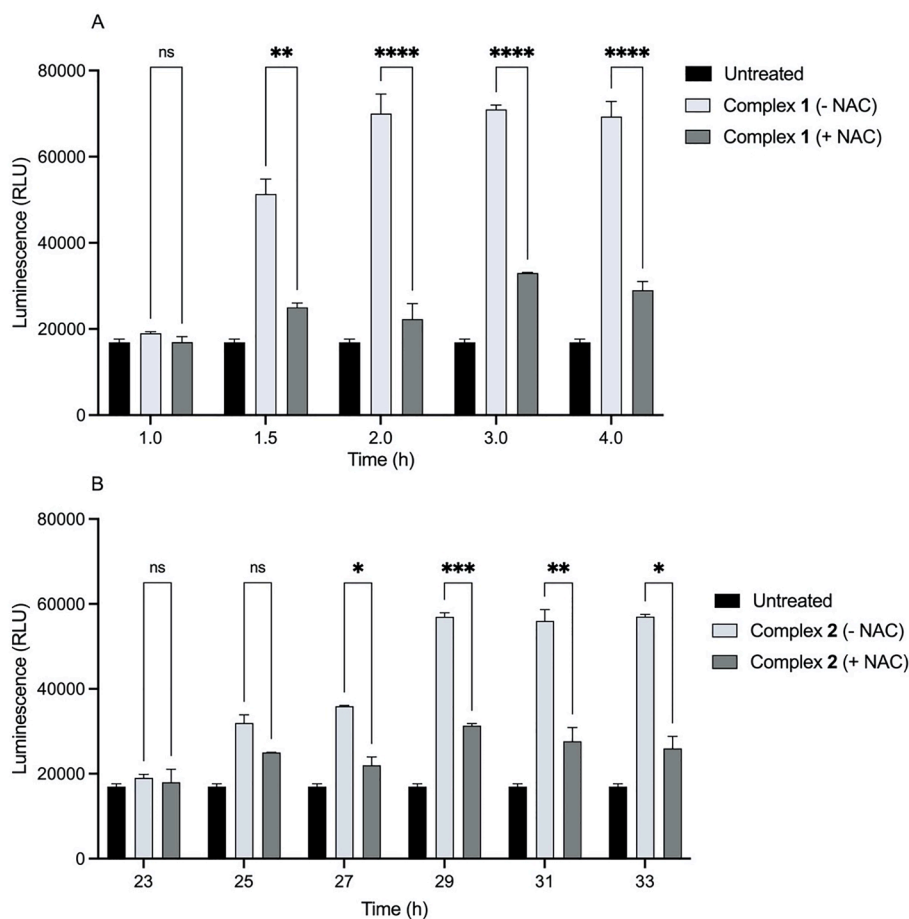


Fig. 12. Caspase 3/7 activity in the MDA-MB-231 VIM RFP cells in the presence and absence of NAC after treatment with complex 1 (A) and complex 2 (B). Cells were seeded at 1.5×10^4 cells per well, then after 24 h incubation, 3000 μM of NAC was added 2 h before treatment with the IC_{50} values of complex 1 (17.5 μM) and complex 2 (5.6 μM). Luminescent Caspase-Glo® 3/7 assay was used at different times by adding the reagent and luminescence was measured by using a plate reader. Values represent the mean \pm SE ($n = 3$). The two-way ANOVA was performed using GraphPad Prism 9 software. (ns = not significant, * $p < 0.05$, ** $p < 0.01$, *** $p < 0.001$, **** $p < 0.0001$).

apoptosis [99]. On the other hand, the cancer cells treated with the IC_{50} value of cisplatin (22.17 μM) did not show caspase 3/7 activity up to 48 h after treatment with the respective data shown in Fig. S6. The cytotoxicity of cisplatin has been linked to DNA binding, which is followed by single-stranded DNA breakage [117]. The specific binding of cisplatin

to 1, 2-intrastrand cross-links of purine bases blocks cell division of cancer cells [118].

To determine the effect of caspase activation on viability, cell viability studies were carried out in the presence and absence of a pan-caspase inhibitor z-VAD-FMK. In the presence of z-VAD-FMK, an

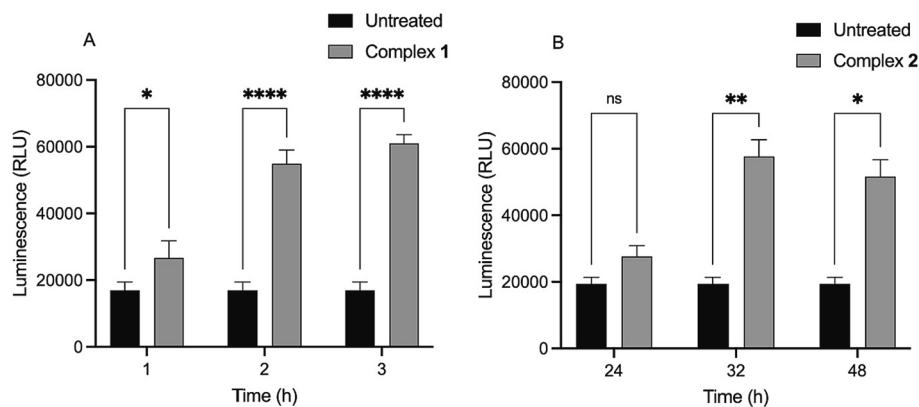


Fig. 13. Caspase 9 activity in the MDA-MB-231 VIM RFP cells after treatment with complex 1 (A) and complex 2 (B) at different time points. The cells were seeded at a density of 1.5×10^4 cells per well followed by adding the IC_{50} value of complex 1 (17.5 μ M) and complex 2 (5.6 μ M). The caspase 9 activity was measured by reading the luminescence at different course times after adding the reagent of the Caspase-Glo® 9 assay. Values represent the mean \pm SE ($n = 3$), and data were analyzed using GraphPad Prism 9 software. (* $p < 0.05$, ** $p < 0.01$, **** $p < 0.0001$).

increase in cell viability was observed in MDA-MB-231 VIM RFP cells exposed to complex 1, with the calculated IC_{50} value almost doubling to $40.3 \pm 1.7 \mu$ M as shown in Fig. 11A. The data indicate that complex 1 induced a caspase-dependent, apoptotic cell death. This resonates with a previous report of the caspase-dependent apoptotic cell death mechanism of complex 1 in the 4 T1-luc cancer cells, where the presence of z-VAD-FMK caused an increased cell viability giving almost a doubling IC_{50} value compared to the IC_{50} value in the absence of caspase inhibitor at 24 h of treatment [89]. For complex 2, there was a significant dose-dependent decrease in cell viability with and without the caspase inhibitor giving very low and close IC_{50} values as shown in Fig. 11B. This implies that the complex induced a non-caspase-dependent cell death mechanism and further buttresses the fact that apoptosis is not the only cell death mechanism employed by complex 2 in MDA-MB-231 VIM RFP cancer cells. Complex 2 induced another cell death mechanism which is suggested to be DNA cleavage based on our results.

The results of caspase 3/7 activity and ROS generation showed induction simultaneously between 1 and 2 h after treatment with the IC_{50} value of complex 1. To study if these two cell death mechanisms, apoptosis and ROS production, were dependent events, caspase 3/7 activity was carried out in the presence and absence of NAC. As such, 3000 μ M of NAC was added to the MDA-MB-231 VIM RFP cells 2 h before treatment with the IC_{50} value of complex 1, then the caspase 3/7 activity was measured at different times using a luminescent Caspase-Glo® 3/7 assay. The results showed that complex 1 induced caspase 3/7 activity both in the presence and absence of NAC as shown in Fig. 12A.

The activity was however reduced in the presence of NAC. These data indicate that complex 1 induced apoptosis *via* ROS formation. Therefore, complex 1 induced caspase- and ROS-dependent cell death mechanisms. Complex 2 also showed activation of caspase 3/7 and ROS production at the same time between 22 and 33 h of treatment. Activation of caspase 3/7 was complete at 29 h of treatment, and its activity was reduced significantly in the presence of NAC as shown in Fig. 12B. The data indicate that ROS production plays a role in inducing apoptosis to kill the MDA-MB-231 VIM RFP cancer cells.

3.3.2.2. Caspase 9 activity to determine apoptotic pathways. Apoptosis is activated primarily through two signaling pathways: receptor-dependent (extrinsic) and mitochondria-dependent (intrinsic). Caspase 8 is involved in the extrinsic pathway, while caspase 9 is involved in the intrinsic pathway [119]. Caspase 9 was studied to investigate which apoptotic pathway was induced after treatment with the complexes. The cancer cells were treated with the IC_{50} values of complexes, then caspase 9 activity was measured by using a luminescent Caspase-Glo® 9 assay. The results showed that both complex 1 and complex 2 activated caspase 9 when compared to untreated cells as shown in Fig. 13. This indicates that both complexes induced apoptosis *via* intrinsic apoptotic pathway in MDA-MB-231-VIM-RFP cell lines.

3.3.3. Caspase 1 activity for pyroptosis cell death detection

Innate immune cells respond to danger signals like ROS production by forming inflammasomes that activate caspase 1 [120]. Caspase 1

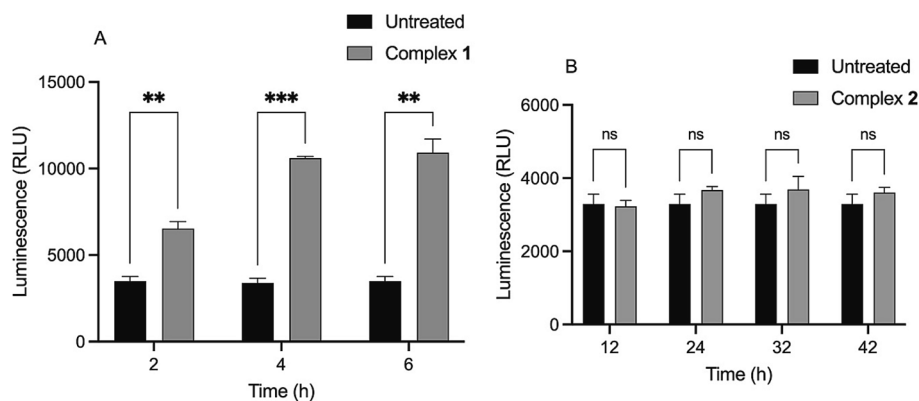


Fig. 14. Caspase 1 activity in the MDA-MB-231 VIM RFP cells after treatment with complex 1 (A) and complex 2 (B) at different time points. The cells were seeded on a 96-well plate (1.5×10^4 cells per well) followed by adding the IC_{50} value of complex 1 (17.5 μ M) and complex 2 (5.6 μ M) at different time points. The caspase 1 activity was measured by adding the reagent of luminescent Caspase-Glo® 1 assay and reading the luminescence with a plate reader. Data were analyzed using GraphPad Prism 9 software. (Data presented as mean + std. err. ** $p < 0.01$, *** $p < 0.001$).

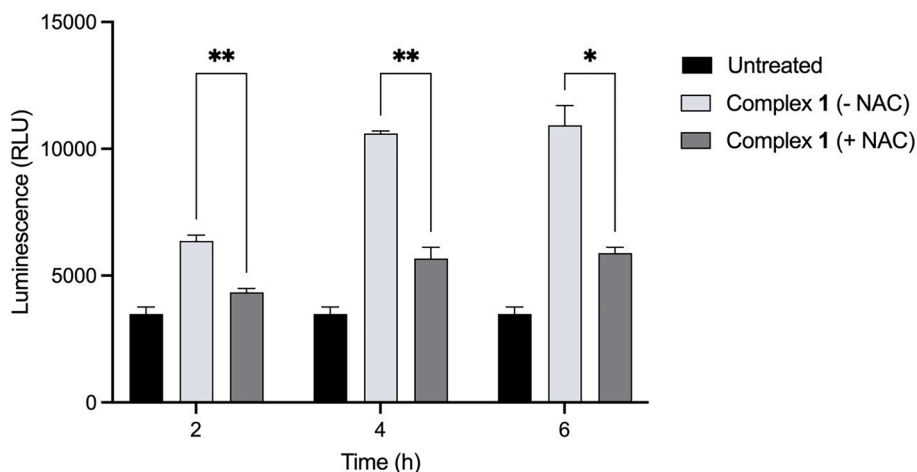


Fig. 15. Caspase 1 activity in the MDA-MB-231 VIM RFP cells after treatment with complex 1 in the presence and absence of NAC. The cells were seeded on a 96-well plate (1.5×10^4 cells per well) followed by adding 3000 μM of NAC 2 h before treatment with the IC_{50} (17.5 μM) value of complex 1 at different time points. The luminescence of solutions was measured after 30 min incubation with the reagent of luminescent Caspase-Glo® 1 assay. The process was carried out in triplicate; then the data was analyzed using GraphPad Prism 9 software through a two-way ANOVA test. (Data presented as mean + std. err. * $p < 0.05$, ** $p < 0.01$).

activates the pyroptosis cell death mechanism which occurs by the formation of plasma membrane pores to release cellular ions allowing water influx. This causes cell swelling, membrane damage, and cell lysis [121,122]. Caspase 1 was detected by using a luminescent Caspase-Glo® 1 reagent after treatment with the IC_{50} values of complexes. The results showed a significant increase in caspase 1 after 2, 4, and 6 h of treatment with complex 1 as shown in Fig. 14A. These results indicate that complex 1 induced pyroptosis cell death mechanism by activation of caspase 1. The results did not show activation in caspase 1 after treatment with complex 2 as shown in Fig. 14B. These results indicate that complex 2 did not induce the pyroptosis cell death mechanism to kill cancer.

To determine if ROS production led to caspase 1 activation, we studied caspase 1 activity in the presence and absence of NAC. 3000 μM of NAC was added to the MDA-MB-231 VIM RFP cells 2 h before treatment with the IC_{50} value of complex 1; then the caspase 1 activity was measured at different times using a luminescent Caspase-Glo® 1 assay. The results showed that complex 1 in the absence of NAC induced caspase 1, but its activity was reduced in the presence of NAC as shown in Fig. 15. The data indicate that ROS production plays a role in the induction of caspase 1 leading to activation of pyroptosis in the MDA-MB-231 VIM RFP cancer cells.

3.3.4. Mitochondrial function and glycolytic rate studies

Mitochondria are often described as an essential target for anti-cancer complexes as they play a crucial role in the regulation of cell energy [123]. Glycolysis and mitochondrial oxidative phosphorylation are the main energy metabolic pathways that serve all other cellular functions [124,125]. Seahorse analyzer allows the measurement of the oxygen consumption rate (OCR) which indicates the oxidative phosphorylation pathway and the extracellular acidification rate (ECAR) which indicates the rate of glycolysis [126]. Glucose is metabolized into lactic acid in the anaerobic glycolysis process generating ATP and releasing protons [127]. In oxidative phosphorylation, the electrons that are produced from NADH are donated to complex I (NADH dehydrogenase) of the electron transport chain (ETC), and then these electrons flow to complex IV (cytochrome *c* oxidase) where oxygen is consumed as the final electron acceptor to generate a molecule of water [128–130]. This electron transport process creates a proton gradient in the inter-membrane space allowing protons to flow back into the matrix through complex V (ATP synthase), causing ATP production [131]. The Seahorse XF Cell Mito Stress Test uses four components, including oligomycin which inhibits complex V of the ETC, leading to a reduction in OCR or ATP generation [132]. The second component is carbonyl cyanide-4

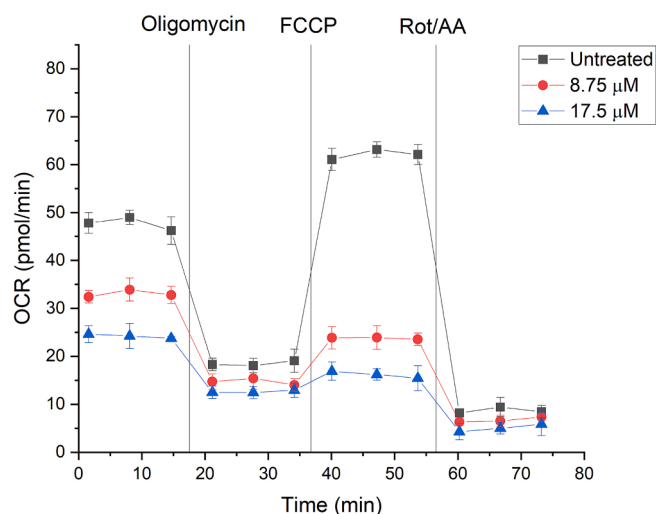


Fig. 16. Effect of complex 1 on the oxygen consumption rate (OCR) in MDA-MB-231 VIM RFP cells. Seahorse XF Cell Mito Stress Test results profile showing relative responses to the addition of oligomycin, FCCP, and rotenone/antimycin A (Rot/AA). The OCR was measured for untreated cells (control), treated cells with 8.75 μM and 17.5 μM values of complex 1 by using an Agilent Seahorse XF analyzer. After 1 h of treatment, the oligomycin (1.5 μM), FCCP (1 μM), and rotenone/antimycin A (0.5 μM) were loaded in the injection ports on the sensor cartridge. The Seahorse XF analyzer was set up for running the mitochondrial stress test assay. The data were analyzed using the Origin 7.0 software.

(trifluoromethoxy) phenylhydrazine (FCCP) which allows protons to move into the mitochondrial matrix leading to an increase in the movement of electrons through the ETC to its maximum speed and respiratory potential [133–135]. The final two components are rotenone and antimycin A which inhibit complexes I (NADH dehydrogenase) and complex III (cytochrome *c* reductase), respectively leading to complete inhibition of ETC [136].

The MDA-MB-231 VIM RFP cells were treated with two different concentrations of complex 1. After 1 h of treatment, the Seahorse XF Cell Mito Stress Test was assayed by adding the four mitochondrial stress components. The results showed an overall reduced oxygen consumption rate profile after treatment with complex 1 compared to untreated cells as shown in Fig. 16.

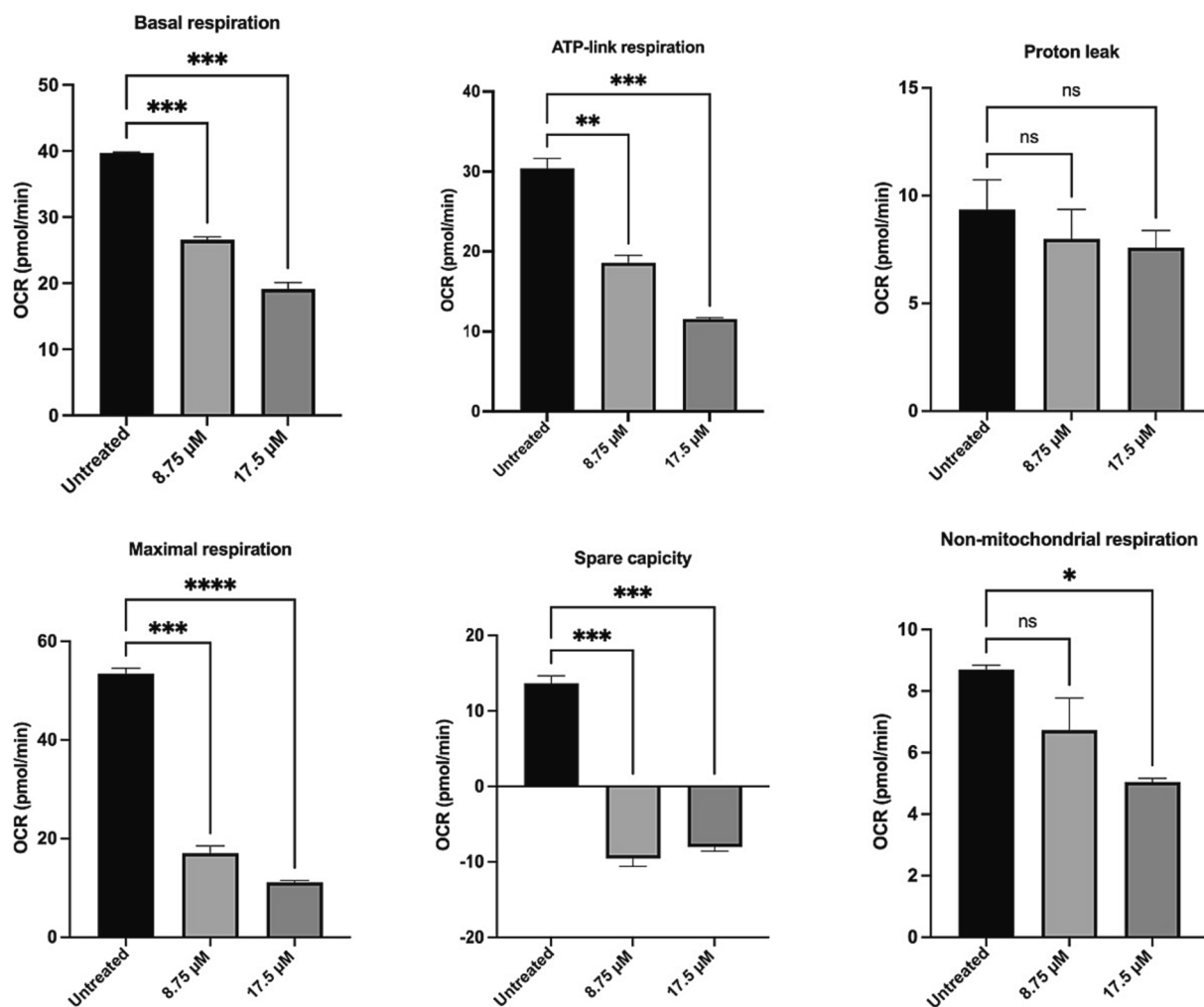


Fig. 17. Quantified results representing relative OCR levels in MDA-MB-231 VIM RFP cells after treatment with 8.75 μ M and 17.5 μ M values of complex 1. The data of OCR level in different types of respiration were calculated and analyzed using GraphPad Prism 9 software. (Data presented as mean + std. err. * p < 0.05, ** p < 0.01, *** p < 0.001, **** p < 0.0001).

From the quantified results (as shown in Fig. 17), a significant decrease in OCR in basal respiration was observed after treatment with complex 1. After adding oligomycin, the ATP synthase was inhibited and complex 1 decreased this ATP-linked respiration. On the other hand, there was no significant alteration in proton leak (oligomycin insensitive respiration) in OCR with and without treatment, which could be due to complex 1 being dependent on the inhibition of the ATP synthase complex. After adding FCCP, OCR was significantly increased in untreated MDA-MB-231 VIM RFP cells showing the maximum respiration that the cells can achieve due to increasing electron transport through the ETC, but complex 1 showed a significant decrease in the maximum respiration which could be a sign of mitochondria damage. Moreover, the spare capacity also showed a significant decrease after treatment with complex 1 through inhibition of the ability of cells to synthesize more ATP than in normal conditions. After adding rotenone and antimycin A (Rot/AA), a decrease in OCR was observed with the IC₅₀ (17.5 μ M) of complex 1 when compared to the untreated group. Thus, complex 1 also inhibited some processes or enzymes that consume oxygen within the cancer cells.

The overall results indicate the inhibition of mitochondrial respiration with complex 1. Disruptions in the mitochondria often lead to increases in caspase 3/7 activity and regulation of apoptotic signals that originate from the intrinsic pathway [137,138]. Based on the evidence presented here, complex 1 induced oxidative stress via ROS overproduction, followed by disruption of the oxidant-antioxidant system

balance, impaired mitochondria function, and finally activation of the intrinsic apoptosis pathway.

The results of Seahorse XF Cell Mito Stress Test assay was used to explain the extracellular acidification rate (ECAR). Fig. 18 shows the effect of complex 1 on the glycolytic rate in MDA-MB-231 VIM RFP cells. After adding oligomycin, the ECAR for both untreated and treated cells was increased compared to the basal condition. Rotenone and antimycin A also caused a high increase in the glycolytic rate due to the complete inhibition of mitochondrial respiration. However, the treatment with complex 1 showed higher ECAR than the cells without treatment indicating that the glycolysis was increased to produce more ATP due to the mitochondria damage and inhibition of mitochondrial respiration that observed with complex 1.

3.3.5. Cell cycle studies

The cell cycle is the process a cell goes through to replicate all of its genetic material and divide into two identical cells [139]. The cell cycle is divided into discrete phases: G1 phase where the cell increases in size and cellular contents are duplicated, DNA synthesis in the S phase, G2 phase where organelles and proteins develop in preparation for cell division, and mitosis which is characterized by the formation of bipolar mitotic spindles, cell separation, and generation of two identical daughter cells [140]. Cell cycle arrest is a point where the cell cycle stops and the processes involved in cell duplication and division are no longer occurring [141].

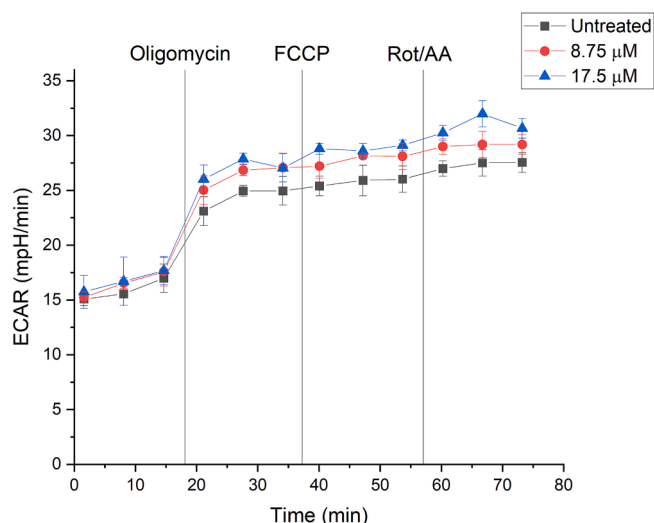


Fig. 18. Effect of complex 1 on the extracellular acidification rate (ECAR) in MDA-MB-231 VIM RFP cells. The cells were plated at 2×10^4 cells/80 μ L in the Seahorse XF cell culture microplate. Then the cells were treated with 8.75 μ M and 17.5 μ M values of complex 1. After 1 h of treatment, the mitochondrial stress test assay was run by adding oligomycin (1.5 μ M), FCCP (1 μ M), and rotenone/antimycin A (0.5 μ M) using the Agilent Seahorse XF analyzer. The data were analyzed using the Agilent Cell Analysis website and collected using Origin 7.0 software.

The cell cycle analysis was performed against the cancer MDA-MB-231 VIM RFP cells by flow cytometry with complex 2 for 24 h using DAPI stain. After treatment of cancer cells with complex 2 (5.63 μ M), there was a significant increase in S phase compared to the control (untreated cells) as shown in Figs. 19 and 20. These results clearly showed that complex 2 induced the growth arrest of cancer cells in S phase from 22.1 % in the control to 40.4 % for complex 2. The corresponding reduction in G1 phase was also obtained (53.0 % in the untreated group to 38.8 % for complex 2) and G2 phase (24.9 % in the control to 18.3 % for complex 2). DNA damage has been reported to induce G1/S phase cell cycle arrest [142]. Complex 2 induced S phase cell cycle arrest in this study might be due to DNA damage as evidenced by its DNA cleavage activity. Topoisomerase inhibitors are potent anti-cancer agents as they induce DNA damage which can result in cell cycle arrest [143]. Topoisomerase inhibitors have thus been implicated as agents inducing S phase arrests [144]. Complex 2, in our previous

study, was reported as an inhibitor of human topoisomerase II α , which participates in DNA replication (S phase) during the cell cycle [90]. The results suggest that complex 2 induced cancer cell death *via* the inhibition of topoisomerase II α , which leads to DNA damage, cell cycle arrest, and subsequent cell death. S phase cell cycle arrest arises in response to DNA damage, thus the S phase arrest herein observed is in response to DNA cleavage induced by complex 2 which ultimately leads to cell death. This is in line with reports of copper complexes which have shown S phase cell cycle arrest [145,146]. Complex 2 thus inhibited cell proliferation in MDA-MB-231 VIM RFP *via* cell cycle arrest.

In this study, an interesting and significant finding is that complex 1 which has a Co(III) metal centre was found to exhibit selective toxicity for breast cancer cells over normal breast cells; while complex 2 is less selective showing similar toxicity to both cancer and non-cancer cells. Now inert Co(III) complexes have been investigated due to their ability to coordinate and inactivate cytotoxic ligands and circulate intact through the bloodstream without affecting healthy tissues [147]. High concentrations of cellular reducing agents, such as reduced nicotinamide adenine dinucleotide phosphate (NADPH), reduced glutathione (GSH), and the hydrogenascorbate anion (which is predominant at physiological conditions [148]), are present in hypoxic tissues and can activate the complex by reduction of the Co(III) metal centre to a labile Co(II) metal centre [147]. It is possible that upon reduction, the release of the active cytotoxic agents (phen and MeATSC) is facilitated due to the labile character of the Co(II) centre. We believe that selective dissociation of the cytotoxin in hypoxic tissues is enhanced by a fast $\text{Co}^{2+}/\text{Co}^{3+}$ reoxidation in healthy tissues, due to higher concentrations of oxygen in normoxic cells [149]. As such, we believe that the selectivity of complex 1 can also be achieved by the reoxidation of Co(II) to the inert Co(III) in non-cancer cells [150,151].

On the other hand, we believe that complex 2 can directly damage DNA, and that the reduction of Cu(II) to Cu(I) can occur in the presence of intracellular thiols, such as reduced glutathione (GSH). As reported in the literature, reduced GSH and Cu(II) interactions has the potential to increase copper-dependent DNA cleavage, most likely through the redox cycling of a "possible" stable copper-DNA complex [152–154]. In the presence of oxygen, Cu(I) can be reoxidised to Cu(II) producing detrimental levels of ROS that are likely not cell type specific [155].

Moreover, complex 2 contains a thiazole moiety in the thiosemicarbazone ligand, where the nitrogen-based heterocycles are structurally important in drug development. The predominant fate of the thiazole ring could be due to oxidative ring scission which is catalysed by CYP450 and the formation of the corresponding α -dicarbonyl

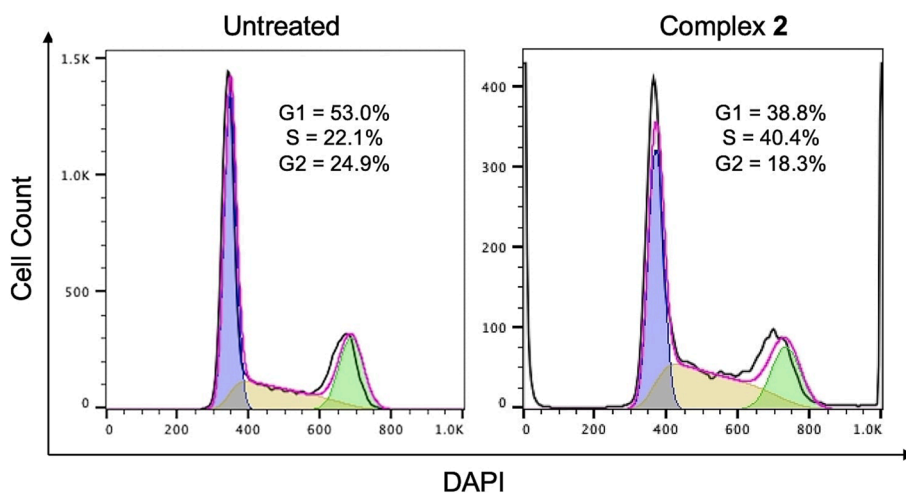


Fig. 19. Cell cycle analysis after treatment with complex 2 for 24 h. The MDA-MB-231 VIM RFP cells were plated at a density of 1×10^6 in 6-well plate. The cells were treated with the IC_{50} of complex 2 (5.63 μ M) for 24 h. The cell cycle was evaluated by flow cytometry using DAPI staining, and its fluorescent was read at 450/50 nm. The fractions of cell cycle (G1, S, and G2) were quantified with the FlowJo software.

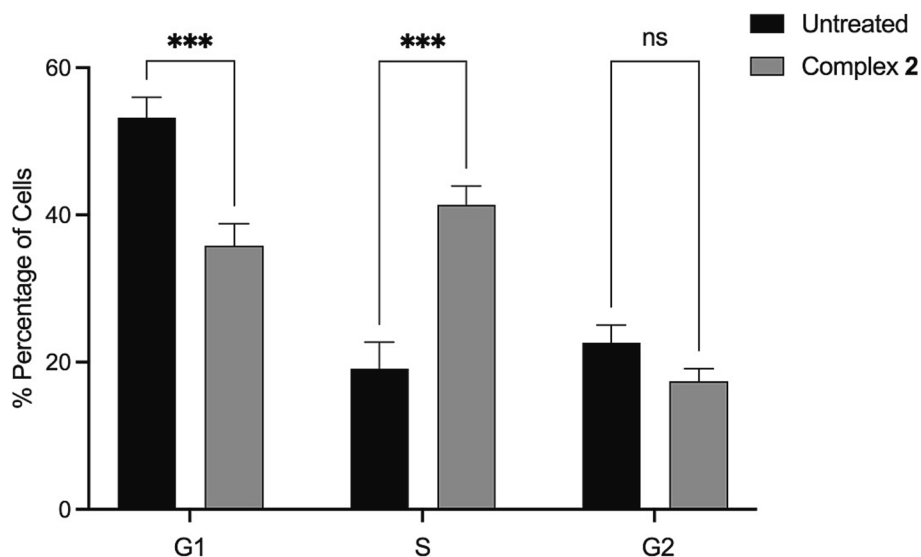


Fig. 20. Quantified results representing fractions of cell cycle (G1, S, and G2) in MDA-MB-231 VIM RFP cells after treatment with complex 2 for 24 h. Experiments were performed in triplicate. The results were analyzed using GraphPad Prism 9 software. (Data presented as mean + std. err. *** $p < 0.001$).

metabolites and thioamide derivatives [156,157]. The well-established toxicity associated with thioamides and thioureas has led to the speculation in the literature that thiazole toxicity is attributed to ring scission yielding the corresponding thioamide metabolite thioureas [158]. This could account for the non-selective nature of complex 2.

As reported in the latest decades, considerable progress has been made in anticancer agents development, and several new anti-cancer agents of natural and synthetic origin have been produced. A review as written by Sharma *et al.* [159] mentioned that among heterocyclic compounds, a thiazole, a five-membered unique heterocyclic motif containing sulphur and nitrogen atoms, can serve as an essential core scaffold in several medicinally important compounds [159]. Thus, a thiazole nucleus is a fundamental part of some clinically applied anti-cancer drugs, such as dasatinib, dabrafenib, ixabepilone, patellamide A, and epothilone [159].

Also, complexes containing thiazoles are more stable because of the strength of the binding between these heteroatoms and DNA [160–162]. Complex 2 was toxic to both cancer and non-cancer cells could be a result of its interaction with the DNA causing DNA damage and affecting healthy cells as well. Complex 2 was reported to be poison inhibitor of human topoisomerase II α , which may account for the observed anti-cancer effects [90]. Complex 2 also was found to extensively cause DNA cleavage in this study when compared to complex 1.

Quite interestingly, thiazole-containing compounds have been utilised as possible inhibitors of several biological targets, including enzyme-linked receptor(s) located on the cell membrane, (i.e., polymerase inhibitors) and the cell cycle (i.e., microtubular inhibitors) [159]. As such, thiazole-containing compounds have been proven to exhibit high effectiveness, potent anti-cancer activity, and less toxicity to non-cancer cells (not the case for our complex 2) [159].

Furthermore, the biological properties of complexes 1 and 2 were determined by their mechanism of action inside the cancer cells. While both complexes 1 and 2 activated caspase 3/7, complex 2 required more than 24 h for peak caspase 3/7 activity while complex 1 activated caspase 3/7 by 2 h. The delayed activity of caspase 3/7 after treatment with complex 2 suggests that the activation of caspase 3/7 in response to complex 2 may be a result of cell death rather than a cause of cell death. In contrast, complex 1 activated apoptosis rapidly through the intrinsic pathway, which is more in pace with a physiological programmed cell death, which ultimately prepares the apoptotic site for tissue repair [163,164]. Many studies have demonstrated that cancer cells are more sensitive than healthy cells to apoptosis through the mitochondrial ROS-

mediated death pathway [165,166]. These findings imply that the anti-cancer drugs that produce ROS inside the mitochondria kill cancer selectively. Therefore, complex 1 showed induction of apoptosis and targeting the mitochondrial energy production, which may account for the selective nature of complex 1. To understand the difference more fully in the selectivity of the two complexes, it will be necessary to investigate the effects of the complexes more specifically on the non-cancer breast cells.

4. Conclusions

This study showed that complexes 1 and 2 were cytotoxic toward the TNBC cell line, MDA-MB-231 VIM RFP. Complex 1 was selectively cytotoxic to cancer cells as it had a higher IC₅₀ value in the non-cancer cell line, MCF-10A, compared to the TNBC cell line. Complex 2 was however toxic to both cancer and non-cancer cells showing that it is not selective. Complex 1 induced apoptosis *via* the intrinsic apoptotic pathway through mitochondrial dysfunction triggered by ROS production. Moreover, the pyroptosis cell death mechanism was also induced by ROS production through treatment with complex 1. On another hand, complex 2 showed a significant DNA cleavage directly after its administration to the plasmid pUC18 DNA. It induced cell cycle arrest in the S phase suggesting that the induction of DNA cleavage occurred *via* topoisomerase II α inhibition. Complex 2 also induced cell death by ROS and the intrinsic apoptotic pathway which occurred later after 24 h of treatment. Hence, while the two complexes induced cell death in the MDA-MB-231 VIM RFP cells, only complex 1 was selectively toxic to cancer cells. There is therefore a need to modify the structure of complex 2 to make it selectively toxic to cancer cells.

CRediT authorship contribution statement

Duaa R. Alajroush: Data curation, Formal analysis, Methodology, Writing – original draft, Writing – review & editing. **Chloe B. Smith:** Data curation, Formal analysis, Investigation, Methodology, Validation. **Brittney F. Anderson:** Data curation, Formal analysis, Investigation, Methodology, Validation, Visualization. **Ifoluwa T. Oyeyemi:** Formal analysis, Methodology. **Stephen J. Beebe:** Conceptualization, Formal analysis, Resources, Software, Supervision, Writing – review & editing. **Alvin A. Holder:** Conceptualization, Formal analysis, Funding acquisition, Investigation, Methodology, Project administration, Resources, Supervision, Validation, Visualization, Writing – original draft, Writing

– review & editing.

Declaration of competing interest

The authors declare the following financial interests/personal relationships which may be considered as potential competing interests: Alvin A. Holder reports a relationship with National Institutes of Health that includes: funding grants.

Data availability

Data will be made available on request.

Acknowledgements

AAH would like to dedicate this publication to my friend, the late Prof. David Richens and his widow, Mrs. Alicia Richens. Prof. Richens, who passed away on Father's Day, June 20, 2021, R.I.P. Research reported in this publication was supported by the National Institute of General Medical Sciences of the National Institutes of Health under Award Number T34GM118259. The content is solely the responsibility of the authors and does not necessarily represent the official views of the National Institutes of Health. Matching funds from Old Dominion University is also acknowledged. This work was also supported by a Saudi Arabian Cultural Mission (SACM) scholarship to DRA. Finally, AAH would like to thank Dr. Mirto Mozzon and his team for allowing us to compile a special issue in honour of Prof. David Richens in the journal, *Inorganica Chimica Acta*.

Appendix A. Supplementary data

Supplementary data to this article can be found online at <https://doi.org/10.1016/j.ica.2023.121898>.

References

- [1] W.D. Foulkes, I.E. Smith, J.S. Reis-Filho, *New Eng. J. Med.* 363 (2010) 1938–1948.
- [2] F. Kassam, K. Enright, R. Dent, G. Dranitsaris, J. Myers, C. Flynn, M. Fralick, R. Kumar, M. Clemons, *Clin. Breast Cancer* 9 (2009) 29–33.
- [3] Y.-R. Liu, Y.-Z. Jiang, X.-E. Xu, X. Hu, K.-D. Yu, Z.-M. Shao, *Clin. Cancer Res.* 22 (2016) 1653–1662.
- [4] H. Ma, G. Ursin, X. Xu, E. Lee, K. Togawa, L. Duan, Y. Lu, K.E. Malone, P. A. Marchbanks, J.A. McDonald, M.S. Simon, S.G. Folger, J. Sullivan-Halley, D. M. Deapen, M.F. Press, L. Bernstein, *Breast Cancer Res.* 19 (2017) 6.
- [5] C.K. Anders, R. Johnson, J. Litton, M. Phillips, A. Bleyer, *Semin. Oncol.* 36 (2009) 237–249.
- [6] T.C. de Ruijter, J. Veeck, J.P. de Hoon, M. van Engeland, V.C. Tjan-Heijnen, *J. Cancer Res. Clin. Oncol.* 137 (2011) 183–192.
- [7] E.C. Dietze, C. Sistrunk, G. Miranda-Carboni, R. O'Regan, V.L. Seewaldt, *Nat. Rev. Cancer* 15 (2015) 248–254.
- [8] F. Bertucci, P. Finetti, N. Cervera, B. Esterni, F. Hermitte, P. Viens, D. Birnbaum, *Int. J. Cancer* 123 (2008) 236–240.
- [9] E.A. Rakha, J.S. Reis-Filho, I.O. Ellis, *J. Clin. Oncol.* 26 (2008) 2568–2581.
- [10] J. Reis-Filho, A. Tutt, *Histopathology* 52 (2008) 108–118.
- [11] A.N. Alexopoulou, C.M. Ho-Yen, V. Papalazarou, G. Elia, J.L. Jones, K. HodiVala-Dilke, *BMC Cancer*, 14 (2014) 237/231–237/238.
- [12] S. Kulkarni, K. Augoff, L. Rivera, B. McCue, T. Khoury, A. Groman, L. Zhang, L. Tian, K. Sossey-Alaoui, *PLoS ONE* 7 (2012) e42895.
- [13] T. Tot, *Cancer* 110 (2007) 2551–2560.
- [14] R. Dent, M. Trudeau, K.I. Pritchard, W.M. Hanna, H.K. Kahn, C.A. Sawka, L. A. Lickley, E. Rawlinson, P. Sun, S.A. Narod, *Clin. Cancer Res.* 13 (2007) 4429–4434.
- [15] C.M. Perou, T. Sorlie, M.B. Eisen, M. Van De Rijn, S.S. Jeffrey, C.A. Rees, J. R. Pollack, D.T. Ross, H. Johnsen, L.A. Akslen, *Nature* 406 (2000) 747–752.
- [16] L. Vona-Davis, D.P. Rose, H. Hazard, M. Howard-McNatt, F. Adkins, J. Partin, G. Hobbs, *Cancer Epidemiol. Prev. Biomarkers* 17 (2008) 3319–3324.
- [17] C. Anders, L.A. Carey, *Oncol. Rep.* 22 (2008) 1233.
- [18] U. Ndagi, N. Mhlongo, M.E. Soliman, *Drug Des. Devel. Ther.* 11 (2017) 599.
- [19] A.K. Renfrew, *Metallomics* 6 (2014) 1324–1335.
- [20] V. Brabec, O. Nováková, *Drug Resist. Updat.* 9 (2006) 111–122.
- [21] M. Frezza, S. Hindo, D. Chen, A. Davenport, S. Schmitt, D. Tomco, Q. Ping Dou, *Curr. Pharm. Des.* 16 (2010) 1813–1825.
- [22] S. Dasari, P.B. Tchounwou, *Eur. J. Pharmacol.* 740 (2014) 364–378.
- [23] B. Rosenberg, L. Vancamp, J.E. Trosko, V.H. Mansour, *Nature* 222 (1969) 385–386.
- [24] E. Wong, C.M. Giandomenico, *Chem. Rev.* 99 (1999) 2451–2466.
- [25] I. Arany, R.L. Safirstein, *Semin. Nephrol.* 23 (2003) 460–464.
- [26] R. Safirstein, J. Winston, M. Goldstein, D. Moel, S. Dikman, J. Guttenplan, *Am. J. Kidney Dis.* 8 (1986) 356.
- [27] I. Kostova, *Recent Pat. Anti-Cancer Drug Discov.* 1 (2006) 1–22.
- [28] C. Monneret, *Ann. Pharm. Fr., Elsevier*, 2011, pp. 286–295.
- [29] B.A. Chan, J.I. Coward, *J. Thorac. Dis.* 5 (2013) S565.
- [30] M. Galanski, V.B. Arion, M.A. Jakupec, B.K. Keppler, *Curr. Pharm. Des.* 9 (2003) 2078–2089.
- [31] M.A. Jakupec, M. Galanski, B.K. Keppler, *Rev. Physiol., Biochem. Pharm.* 146 (2003) 1–54.
- [32] L.G. Eng, S. Dawood, R. Dent, *Curr. Opin. Support Palliat. Care* 9 (2015) 301–307.
- [33] S. Lewis, J. Yee, S. Kilbreath, K. Willis, *Breast* 24 (2015) 242–247.
- [34] P. Wheatley-Price, M. Ali, K. Balchin, J. Spencer, E. Fitzgibbon, C. Cripps, *Curr. Oncol.* 21 (2014) 187–192.
- [35] H. Calvert, I. Judson, W. Van der Vijgh, *Cancer Surv.* 17 (1993) 189–217.
- [36] I. Ott, R. Gust, *Int. J. Pharm. Med. Chem.* 340 (2007) 117–126.
- [37] I. Ott, *Coord. Chem. Rev.* 253 (2009) 1670–1681.
- [38] A. Bergamo, G. Sava, *Dalton Trans.* 40 (2011) 7817–7823.
- [39] I. Kostova, *Anti-Cancer Agents Med. Chem.* 9 (2009) 827–842.
- [40] A. Bergamo, C. Gaiddon, J.H.M. Schellens, J.H. Beijnen, G. Sava, *J. Inorg. Biochem.* 106 (2012) 90–99.
- [41] C.R. Chitambar, *Future Med. Chem.* 4 (2012) 1257–1272.
- [42] M.D. Hall, T.W. Failes, N. Yamamoto, T.W. Hambley, *Dalton Trans.* (2007) 3983–3990.
- [43] R.-W.-Y. Sun, D.-L. Ma, E.-L.-M. Wong, C.-M. Che, *Dalton Trans.* (2007) 4884–4892.
- [44] L.A. Onambele, N. Hoffmann, L. Kater, L. Hemmersbach, J.-M. Neudörfel, N. Sitnikov, B. Kater, C. Frias, H.-G. Schmalz, A. Prokop, *RSC Med. Chem.* (2022).
- [45] S. Rafique, M. Idrees, A. Nasim, H. Akbar, A. Athar, *Biotechnol. Mol. Biol. Rev.* 5 (2010) 38–45.
- [46] M.-J. Davila-Rodriguez, J.P. Barolli, K.M. de Oliveira, L. Colina-Vegas, F. da Silva Miranda, E.E. Castellano, G. Von Poelhsitz, A.A. Batista, *Arch. Biochem. Biophys.* 660 (2018) 156–167.
- [47] D. Havrylyuk, M. Deshpande, S. Parkin, E.C. Glazer, *Chem. Commun.* 54 (2018) 12487–12490.
- [48] A. Kumar, A. Dixit, S. Banerjee, S. Mukherjee, S. Sahoo, A.A. Karande, A. R. Chakravarty, *Indian J. Chem. Sect. A: Inorg. Bio-inorg. Phys. Theor. Anal. Chem.* 57A (2018) 409–417.
- [49] B. Liu, S. Monro, L. Lystrom, C.G. Cameron, K. Colon, H. Yin, S. Kilina, S. A. McFarland, W. Sun, *Inorg. Chem.* 57 (2018) 9859–9872.
- [50] G.-L. Ma, X.-D. Bi, F. Gao, Z. Feng, D.-C. Zhao, F.-J. Lin, R. Yan, D. Liu, P. Liu, J. Chen, H. Zhang, *J. Inorg. Biochem.* 185 (2018) 1–9.
- [51] P. Zhang, H. Huang, *Dalton Trans.* 47 (2018) 14841–14854.
- [52] A.A. Holder, D.F. Zigler, M.T. Tarrago-Trani, B. Storrie, K.J. Brewer, *Inorg. Chem.* 46 (2007) 4760.
- [53] B. Storrie, A. Holder, K.J. Brewer, *Proc. SPIE-Int. Soc. Opt. Eng.* 6139 (2006) 336–342.
- [54] S. Swavey, Z. Fang, K.J. Brewer, *Inorg. Chem.* 41 (2002) 2598–2607.
- [55] R.L. Williams, H.N. Toft, B. Winkel, K.J. Brewer, *Inorg. Chem.* 42 (2003) 4394–4400.
- [56] M.D. Hall, N.K. Salam, J.L. Hellawell, H.M. Fales, C.B. Kensler, J.A. Ludwig, G. Szakacs, D.E. Hibbs, M.M. Gottesman, *J. Med. Chem.* 52 (2009) 3191–3204.
- [57] P.J. Jansson, P.C. Sharpe, P.V. Bernhardt, D.R. Richardson, *J. Med. Chem.* 53 (2010) 5759–5769.
- [58] J. Easmon, G. Puerstinger, G. Heinisch, T. Roth, H.H. Fiebig, W. Holzer, W. Jaeger, M. Jenny, J. Hofmann, *J. Med. Chem.* 44 (2001) 2164–2171.
- [59] L.A. Saryan, E. Ankel, C. Krishnamurti, D.H. Petering, H. Elford, *J. Med. Chem.* 22 (1979) 1218–1221.
- [60] C.R. Kowol, R. Berger, R. Eichinger, A. Roller, M.A. Jakupec, P.P. Schmidt, V. B. Arion, B.K. Keppler, *J. Med. Chem.* 50 (2007) 1254–1265.
- [61] A.I. Matesanz, P. Souza, *Mini-Rev. Med. Chem.* 9 (2009) 1389–1396.
- [62] B.M. Zeglis, V. Divilov, J.S. Lewis, *J. Med. Chem.* 54 (2011) 2391–2398.
- [63] Y. Yu, D.S. Kalinowski, Z. Kovacevic, A.R. Sifafakas, P.J. Jansson, C. Stefani, D. B. Lovejoy, P.C. Sharpe, P.V. Bernhardt, D.R. Richardson, *J. Med. Chem.* 52 (2009) 5271–5294.
- [64] G. Pelosi, *Open Crystallogr. J.* 3 (2010).
- [65] J. Shim, N.R. Jyothi, N.M. Farook, *Asian J. Chem.* 25 (2013) 5838.
- [66] N.P. Prajapati, H.D. Patel, *Synth. Commun.* 49 (2019) 2767–2804.
- [67] N.R. Jyothi, N.M. Farook, M. Cho, J. Shim, *Asian J. Chem.* 25 (2013) 5841.
- [68] D.S. Kalinowski, P. Quach, D.R. Richardson, *Future Med. Chem.* 1 (2009) 1143–1151.
- [69] B.M. Paterson, P.S. Donnelly, *Chem. Soci. Rev.* 40 (2011) 3005–3018.
- [70] P. Heffeter, V.F. Pape, É.A. Enyedy, B.K. Keppler, G. Szakacs, C.R. Kowol, *Antioxid. Redox Signal.* 30 (2019) 1062–1082.
- [71] S.N. Maqbool, S.C. Lim, K.C. Park, R. Hanif, D.R. Richardson, P.J. Jansson, Z. Kovacevic, *Brit. J. Pharmacol.* 177 (2020) 2365–2380.
- [72] B. Shakya, P.N. Yadav, *Rev. Med. Chem.* 20 (2020) 638–661.
- [73] E.L. Chang, C. Simmers, D.A. Knight, *Pharmaceuticals* 3 (2010) 1711.
- [74] C.R. Munteanu, K. Suntharalingam, *Dalton Trans.* 44 (2015) 13796–13808.
- [75] A. Chylewska, M. Biedulska, P. Sumczynski, M. Makowski, *Curr. Med. Chem.* 25 (2018) 1729–1791.
- [76] P.B. Cressey, A. Eskandari, P.M. Bruno, C. Lu, M.T. Hemann, K. Suntharalingam, *ChemBioChem* 17 (2016) 1713–1718.

- [77] P.B. Cressey, A. Eskandari, K. Suntharalingam, *Inorganics*, 5 (2017) 12/11–12/13.
- [78] A.P. King, H.A. Gellineau, J.-E. Ahn, S.N. MacMillan, J.J. Wilson, *Inorg. Chem.* 56 (2017) 6609–6623.
- [79] A.K. Renfrew, E.S. O'Neill, T.W. Hambley, E.J. New, *Coord. Chem. Rev.* 375 (2018) 221–233.
- [80] P. Zhang, P.J. Sadler, *Eur. J. Inorg. Chem.* 2017 (2017) 1541–1548.
- [81] R.W. Leggett, *Sci. Environ.* 389 (2008) 259–269.
- [82] M. Suh, C.M. Thompson, G.P. Brorby, L. Mittal, D.M. Proctor, *Regul. Toxicol. Pharmacol.* 79 (2016) 74–82.
- [83] R. Manikandan, P. Viswanathamurthi, K. Velmurugan, R. Nandhakumar, T. Hashimoto, A. Endo, *J. Photochem. Photobiol., B: Biol.* 130 (2014) 205–216.
- [84] R.A. Festa, D.J. Thiele, *Curr. Biol.*, 21 (2011) R877–R883.
- [85] N. Metzler-Nolte, H. Kraatz, *Concepts and Models in Bioinorganic Chemistry*, Wiley-VCH (2006).
- [86] N.K. Singh, A.A. Kumbhar, Y.R. Pokharel, P.N. Yadav, *J. Inorg. Biochem.* 210 (2020), 111134.
- [87] M. Carcelli, M. Tegoni, J. Bartoli, C. Marzano, G. Pelosi, M. Salvalaio, D. Rogolino, V. Gandin, *Eur. J. Med. Chem.* 194 (2020), 112266.
- [88] D. Palanimuthu, S.V. Shinde, K. Somasundaram, A.G. Samuelson, *J. Med. Chem.* 56 (2013) 722–734.
- [89] S.J. Beebe, M.J. Celestine, J.L. Bullock, S. Sandhaus, J.F. Arca, D.M. Crokep, T. A. Ludvig, S.R. Foster, J.S. Clark, F.A. Beckford, C.M. Tano, E.A. Tonsel-White, R. K. Gurung, C.E. Stankavich, Y.-C. Tse-Dinh, W.L. Jarrett, A.A. Holder, *J. Inorg. Biochem.* 203 (2020), 110907.
- [90] S. Sandhaus, R. Taylor, T. Edwards, A. Huddleston, Y. Wooten, R. Venkatraman, R.T. Weber, A. González-Sarriás, P.M. Martin, P. Cagle, Y.-C. Tse-Dinh, S.J. Beebe, N. Seeram, A.A. Holder, *Inorg. Chem. Commun.* 64 (2016) 45–49.
- [91] S.M. Cohen, S.J. Lippard, (2001).
- [92] J.E. Dewese, N. Osheroff, *Nucleic Acids Res.* 37 (2009) 738–748.
- [93] V. Rajendiran, R. Karthik, M. Palaniandavar, H. Stoeckli-Evans, V.S. Periasamy, M.A. Akbarsha, B.S. Srinaga, H. Krishnamurthy, *Inorg. Chem.* 46 (2007) 8208–8221.
- [94] L.J. Boerner, J.M. Zaleski, *Curr. Opin. Chem. Biol.* 9 (2005) 135–144.
- [95] S. Swavey, K.J. Brewer, *Inorg. Chem.* 41 (2002) 6196–6198.
- [96] L.E. Joyce, J.D. Aguirre, A.M. Angeles-Boza, A. Chouai, P.-K.-L. Fu, K.R. Dunbar, C. Turro, *Inorg. Chem.* 49 (2010) 5371–5376.
- [97] Q.-L. Zhang, J.-G. Liu, H. Chao, G.-Q. Xue, L.-N. Ji, *J. Inorg. Biochem.* 83 (2001) 49–55.
- [98] B. Peng, H. Chao, B. Sun, H. Li, F. Gao, L.-N. Ji, *J. Inorg. Biochem.* 101 (2007) 404–411.
- [99] G.-J. Chen, X. Qiao, P.-Q. Qiao, G.-J. Xu, J.-Y. Xu, J.-L. Tian, W. Gu, X. Liu, S.-P. Yan, *J. Inorg. Biochem.* 105 (2011) 119–126.
- [100] V. Aggarwal, H.S. Tuli, A. Varol, F. Thakral, M.B. Yerer, K. Sak, M. Varol, A. Jain, M. Khan, G. Sethi, *Biomolecules* 9 (2019) 735.
- [101] K.A. Conklin, *Integr. Cancer Ther.* 3 (2004) 294–300.
- [102] J. Chandra, A. Samali, S. Orrenius, *Free Radic. Biol. Med.* 29 (2000) 323–333.
- [103] P. Vandenabeele, L. Galluzzi, T. Vanden Berghe, G. Kroemer, *Nat. Rev. Mol. Cell Biol.* 11 (2010) 700–714.
- [104] K. Sakthikumar, R.W.M. Krause, B.K. Isamura, J.D. Raja, S. Athimoolam, *J. Inorg. Biochem.* 236 (2022), 111953.
- [105] B. Gowdhami, Y. Manojkumar, R. Vimala, V. Ramya, B. Karthiyayini, B. Kadalmani, M.A. Akbarsha, *BioMetals* 35 (2022) 67–85.
- [106] C.H. Ng, T.H. Tan, N.H. Tioh, H.L. Seng, M. Ahmad, S.W. Ng, W.K. Gan, M.L. Low, J.-W. Lai, M. Zulkefeli, *J. Inorg. Biochem.* 220 (2021), 111453.
- [107] M.K. Lesiów, U.K. Komarnicka, K. Stokowa-Sołtys, K. Rolka, A. Łęgowska, N. Ptaszyńska, R. Wiczorek, A. Kyzioł, M. Jeżowska-Bojczuk, *Dalton Trans.* 47 (2018) 5445–5458.
- [108] A. Strbu, O. Palamarcu, M.V. Babak, J.M. Lim, K. Ohui, E.A. Enyedy, S. Shova, D. Darvasiová, P. Rapta, W.H. Ang, *Dalton Trans.* 46 (2017) 3833–3847.
- [109] K.E. Prosser, S.W. Chang, F. Saraci, P.H. Le, C.J. Walsby, *J. Inorg. Biochem.* 167 (2017) 89–99.
- [110] A. Banaspati, D. Das, C.J. Choudhury, A. Bhattacharyya, T.K. Goswami, *J. Inorg. Biochem.* 191 (2019) 60–68.
- [111] M. Sadegh Soltan-Sharifi, M. Mojtahedzadeh, A. Najafi, M. Reza Khajavi, M. Reza Rouini, M. Moradi, A. Mohammadirad, M. Abdollahi, *Hum. Exp. Toxicol.* 26 (2007) 697–703.
- [112] M. Zafarullah, W. Li, J. Sylvester, M. Ahmad, *Cell. Mol. Life Sci.* 60 (2003) 6–20.
- [113] S.W. Lowe, A.W. Lin, *Carcinogenesis* 21 (2000) 485–495.
- [114] C. Trejo-Solis, G. Palencia, S. Zuñiga, A. Rodríguez-Ropon, L. Osorio-Rico, S. Torres Luvia, I. Gracia-Mora, L. Marquez-Rosado, A. Sánchez, M.E. Moreno-García, A. Cruz, M.E. Bravo-Gómez, L. Ruiz-Ramírez, S. Rodríguez-Enriquez, J. Sotelo, *Neoplasia* 7 (2005) 563–574.
- [115] L. Galluzzi, N. Larochette, N. Zamzami, G. Kroemer, *Oncogene* 25 (2010) 4812–4830.
- [116] V. Gogvadze, B. Zhivotovsky, S. Orrenius, *Mol. Aspects Med.* 31 (2010) 60–74.
- [117] V. Cepeda, M.A. Fuertes, J. Castilla, C. Alonso, C. Quevedo, J.M. Pérez, *Anti-Cancer Agents Med. Chem.* 7 (2007) 3–18.
- [118] A. Brown, S. Kumar, P.B. Tchounwou, *J. Cancer Sci. Ther.* 11 (2019).
- [119] L. Li, Y.-S. Wong, T. Chen, C. Fan, W. Zheng, *Dalton Trans.* 41 (2012) 1138–1141.
- [120] R. Medzhitov, C. Janeway Jr, *J. Med. Chem.* 343 (2000) 338–344.
- [121] E.A. Miao, J.V. Rajan, A. Aderem, *Immunol. Rev.* 243 (2011) 206–214.
- [122] T. Arakelian, K. Oosterhuis, E. Tondini, M. Los, J. Vree, M. van Geldorp, M. Camps, B. Teunisse, I. Zoutendijk, R. Arens, *Vaccine* 40 (2022) 2087–2098.
- [123] F. Qi, A. Li, Y. Inagaki, H. Xu, D. Wang, X. Cui, L. Zhang, N. Kokudo, G. Du, W. Tang, *Food Chem. Toxicol.* 50 (2012) 295–302.
- [124] P.M. Herst, A.S. Tan, D.-J.-G. Scarlett, M.V. Berridge, *Biochim. Biophys. Acta* 1656 (2004) 79–87.
- [125] J. Zheng, *Oncol. Lett.* 4 (2012) 1151–1157.
- [126] G.J. Van der Windt, C.H. Chang, E.L. Pearce, *Curr. Protoc. Immunol.*, 113 (2016) 3.16 B. 11–13.16 B. 14.
- [127] X.L. Zu, M. Guppy, *Biochem. Biophys. Res. Commun.* 313 (2004) 459–465.
- [128] D.C. Wallace, *Nat. Rev. Cancer* 12 (2012) 685–698.
- [129] M. Guppy, P. Leedman, X. Zu, V. Russell, *Biochem. J.* 364 (2002) 309–315.
- [130] O. Bergman, D. Ben-Shachar, *Can. J. Psychiatry* 61 (2016) 457–469.
- [131] M.G. Vander Heiden, L.C. Cantley, C.B. Thompson, *Science* 324 (2009) 1029–1033.
- [132] M. Saraste, *Science* 283 (1999) 1488–1493.
- [133] S.M. Jaber, N. Yadava, B.M. Polster, *Exp. Neurol.* 328 (2020), 113282.
- [134] K.A. Grasmick, H. Hu, E.A. Hone, I. Farooqi, S.L. Rellick, J.W. Simpkins, X. Ren, *J. Neuroinfect. Dis.* 9 (2018).
- [135] J.P. Brennan, R. Southworth, R.A. Medina, S.M. Davidson, M.R. Duchon, M. J. Shattock, *Cardiovasc. Res.* 72 (2006) 313–321.
- [136] A.S. Divakaruni, G.W. Rogers, A.N. Murphy, *Curr. Protoc. Toxicol.*, 60 (2014) 25.22. 21–25.22. 16.
- [137] T.T. Renault, J.E. Chipuk, *Chem. Biol.* 21 (2014) 114–123.
- [138] S. Matt, T.G. Hofmann, *Cell. Mol. Life Sci.* (2016).
- [139] E. Israels, L. Israels, *Oncologist* 5 (2000) 510–513.
- [140] G.H. Williams, K. Stoeber, *Curr. Opin. Cell Biol.* 19 (2007) 672–679.
- [141] D. Hanahan, R.A. Weinberg, *Cell* 144 (2011) 646–674.
- [142] F.S. Wyllie, M.F. Haughton, J.A. Bond, J.M. Rowson, C.J. Jones, D. Wynford-Thomas, *Oncogene* 12 (1996) 1077–1082.
- [143] M.N. Drwal, J. Marinello, S.G. Manzo, L.P. Wakelin, G. Capranico, R. Griffith, *PLoS One* 9 (2014) e114904.
- [144] W.A. Cliney, K.A. Lewis, K.K. Lilly, S.H. Kaufmann, *J. Biol. Chem.* 277 (2002) 1599–1606.
- [145] H. Zhang, R. Thomas, D. Oupicky, F. Peng, *J. Biol. Inorg. Chem.* 13 (2008) 47–55.
- [146] S. Arikrishnan, J.S. Loh, X.W. Teo, F. Bin Norizan, M.L. Low, S.H. Lee, J.B. Foo, Y. S. Tor, *Anti-Cancer Agents Med. Chem.* 22 (2022) 999–1011.
- [147] U. Jungwirth, *Antioxid. Redox. Signal.* 15 (2011) 1085–1127.
- [148] A.A. Holder, R.F.G. Brown, S.C. Marshall, V.C.R. Payne, M.D. Cozier, W. A. Alleyne Jr., C.O. Bovell, *Trans. Met. Chem.* 25 (2000) 605–611.
- [149] N. Graf, S.J. Lippard, *Adv. Drug Deliv. Rev.* 64 (2012) 993–1004.
- [150] A.P. King, H.A. Gellineau, S.N. MacMillan, J.J. Wilson, *Dalton Trans.* 48 (2019) 5987–6002.
- [151] M. Kozsup, E. Farkas, A.C. Bényei, J. Kasparkova, H. Crlíkova, V. Brabec, P. Buglyó, *J. Inorg. Biochem.* 193 (2019) 94–105.
- [152] M. Chikira, Y. Tomizawa, D. Fukita, T. Sugizaki, N. Sugawara, T. Yamazaki, A. Sasano, H. Shindo, M. Palaniandavar, W.E. Antholine, *J. Inorg. Biochem.* 89 (2002) 163–173.
- [153] R. Ruiz, B. García, J. García-Tojal, N. Busto, S. Ibeas, J.M. Leal, C. Martins, J. Gaspar, J. Borrás, R. Gil-García, *J. Biol. Inorg. Chem.* 15 (2010) 515–532.
- [154] W. Prütz, *Biochem. J.* 302 (1994) 373–382.
- [155] C.R. Kowol, P. Heffeter, W. Miklos, L. Gille, R. Trondl, L. Cappellacci, W. Berger, B.K. Keppler, *J. Biol. Inorg. Chem.* 17 (2012) 409–423.
- [156] T. Mizutani, K. Yoshida, S. Kawazoe, *Drug Metab. Dispos.* 22 (1994) 750–755.
- [157] T. Mizutani, K. Suzuki, *Toxicol. Lett.* 85 (1996) 101–105.
- [158] D.K. Dalvie, A.S. Kalgutkar, S.C. Khojasteh-Bakht, R.S. Obach, J.P. O'Donnell, *Chem. Res. Toxicol.* 15 (2002) 269–299.
- [159] P.C. Sharma, K.K. Bansal, A. Sharma, D. Sharma, A. Deep, *Eur. J. Med. Chem.* 188 (2020), 112016.
- [160] P. Martins, J. Jesus, S. Santos, L.R. Raposo, C. Roma-Rodrigues, P.V. Baptista, A. R. Fernandes, *Molecules* 20 (2015) 16852–16891.
- [161] O. Ajani, O. Audu, D. Aderhunmu, F. Owolabi, A. Olomieja, *Am. J. Drug Discov. Dev.* 7 (2017) 1–24.
- [162] Y. Özkay, İ. İşıkdağ, Z. İncesu, G. Akalın, *Eur. J. Med. Chem.* 45 (2010) 3320–3328.
- [163] R. Jan, *Adv. Pharm. Bull.* 9 (2019) 205.
- [164] I.K. Poon, C.D. Lucas, A.G. Rossi, K.S. Ravichandran, *Nat. Rev. Immunol.* 14 (2014) 166–180.
- [165] Y. Suzuki-Karasaki, M. Suzuki-Karasaki, M. Uchida, T. Ochiai, *Front. Oncol.* 4 (2014) 128.
- [166] T. Tatsuta, S. Sugawara, K. Takahashi, Y. Ogawa, M. Hosono, K. Nitta, *Front. Oncol.* 4 (2014) 139.